

Spring 5-6-2016

Characterization of a Wind Tunnel for Use in Offshore Wind Turbine Development with Mitigation Measures for the Wall Effect of Proximal Structures

James Newton

University of Maine, james.newton1@maine.edu

Follow this and additional works at: <http://digitalcommons.library.umaine.edu/etd>

 Part of the [Energy Systems Commons](#), [Ocean Engineering Commons](#), and the [Other Mechanical Engineering Commons](#)

Recommended Citation

Newton, James, "Characterization of a Wind Tunnel for Use in Offshore Wind Turbine Development with Mitigation Measures for the Wall Effect of Proximal Structures" (2016). *Electronic Theses and Dissertations*. 2443.

<http://digitalcommons.library.umaine.edu/etd/2443>

This Open-Access Thesis is brought to you for free and open access by DigitalCommons@UMaine. It has been accepted for inclusion in Electronic Theses and Dissertations by an authorized administrator of DigitalCommons@UMaine.

**CHARACTERIZATION OF A WIND TUNNEL FOR USE IN OFFSHORE WIND
TURBINE DEVELOPMENT WITH MITIGATION MEASURES FOR THE
WALL EFFECT OF PROXIMAL STRUCTURES**

By

James Michael Newton

B.S. Rensselaer Polytechnic Institute, 2002

A THESIS

Submitted in Partial Fulfillment of the

Requirements for the Degree of

Master of Science

(in Mechanical Engineering)

The Graduate School

The University of Maine

May 2016

Advisor Committee:

Andrew J. Goupee, Libra Assistant Professor of Mechanical Engineering,

Advisor

Michael L. Peterson, Professor of Mechanical Engineering

Krish P. Thiagarajan, Alston D. and Ada Lee Correll Presidential Chair in

Energy and Professor of Mechanical Engineering

THESIS ACCEPTANCE STATEMENT

On behalf of the Graduate Committee for James Michael Newton I affirm that this manuscript is the final and accepted thesis. Signatures of all committee members are on file with the Graduate School at the University of Maine, 42 Stodder Hall, Orono, Maine.

Dr. Andrew J. Goupee, Libra Assistant Professor of Mechanical Engineering

<Date>

LIBRARY RIGHTS STATEMENT

In presenting this thesis in partial fulfillment of the requirements for an advanced degree at the University of Maine, I agree that the Library shall make it freely available for inspection. I further agree that permission for "fair use" copying of this thesis for scholarly purposes may be granted by the Librarian. It is understood that any copying or publication of this thesis for financial gain shall not be allowed without my written permission.

Signature:

Date:

**CHARACTERIZATION OF A WIND TUNNEL FOR USE IN OFFSHORE WIND
TURBINE DEVELOPMENT WITH MITIGATION MEASURES FOR THE
WALL EFFECT OF PROXIMAL STRUCTURES**

By James Michael Newton

Thesis Advisor: Dr. Andrew J. Goupee

An Abstract of the Dissertation Presented
in Partial Fulfillment of the Requirements for the
Degree of Master of Science
(in Mechanical Engineering)
May, 2016

This thesis supports the development of the Harold Alfond W^2 Ocean Engineering Laboratory constructed at the University of Maine through several investigations conducted with a one-third scale wind generation system. The scale wind generator is first tested in what is considered an open-circuit wind tunnel configuration to determine the influence proximal building walls of a facility housing such a device may have on the consistency and capacity of a wind generator. Turbine performance testing with the wind generator to identify any susceptibility to proximal wall influence is also conducted. This is of interest as the full-scale system will operate in different orientations within a rectangular building. Baseline wind generator performance and test turbine performance data in this configuration is established for use in comparison to alternative tunnel configurations. Additional investigations are carried out to determine the effectiveness of mitigation measures intended to reduce or eliminate any influence of proximal facility walls

on wind generator performance. In these investigations any associated effects on wind generator performance and turbine performance testing must be understood. One alternative to the wind generator configuration is the conversion of the generator to a traditional wind tunnel, also known as a closed-circuit tunnel configuration, where the test flow is collected and reused by the tunnel making it immune to changes in orientation within the building. Active recirculation in the form of a bank of fans placed at the end of the test section is also investigated as an alternative method of masking the effects of nearby facility walls on wind generator and turbine testing performance.

This thesis is organized into 4 chapters. Chapter 1 details the current state of the art of floating offshore wind turbine development; past efforts are discussed along with motivations for future testing endeavors. Chapter 2 outlines the experimental instrumentation and procedures used throughout this body of work. Chapter 3 chronicles the hardware used by the wind generator, its operation, and baseline data collected. Chapter 4 discusses the conversion of the wind generator in chapter 3 to a wind tunnel that is subjected to the same tests and turbine runs as the wind generator in a comparative study. This chapter also tests the sensitivity of the wind generation system, and associated turbine tests, to the intrusion of nearby facility walls. Chapter 4 also investigates the use of active recirculation as a way to mitigate any negative influence of facility infrastructure on the wind generation system. Chapter 5 summarizes the findings of this study.

ACKNOWLEDGEMENTS

I would like to thank my wife Kristin for her unending support and encouragement throughout this effort; without her this would not have been possible. Additionally, I would like to recognize my parents for fostering my sense of curiosity, and encouraging me to pursue higher education.

I would also like to thank my graduate committee for their involvement and guidance throughout the project. Dr. Andy Goupee's insight into offshore wind energy and ongoing support was invaluable. Dr. Mick Peterson was instrumental in my academic guidance as he first introduced me to this project and always remained available for counsel. Dr. Krish Thiagarajan's encouragement and support in pursuit of publishing research findings and conference participation was invaluable. Lastly, I would like to thank Dr. Raul Urbina and Matthew Cameron for all I have learned while collaborating with them. Their technical and analytical expertise along with their willingness to teach me has greatly enriched my educational experience.

I would also like to gratefully acknowledge that this work was made possible through the financial contributions from the University of Maine Mechanical Engineering Department, The National Science Foundation (Award 1337895), and a University of Maine Libra Professorship.

TABLE OF CONTENTS

ACKNOWLEDGEMENTS.....	iii
LIST OF FIGURES	vi
Chapter	
1. FLOATING OFFSHORE WIND TURBINE DEVELOPMENT	1
1.1. Motivations.....	2
1.2. FOWT Design and Analysis.....	2
1.3. Numerical Codes and the Need for Experimental Verification	6
1.4. Experimental Methods	9
1.5. Wind Tunnel Design.....	11
1.6. Testing Facilities and Accomplishments	17
1.7. Test Flow Sensitivity	21
1.8. Development of Future Facilities	22
2. EXPERIMENTAL TESTING PROCEDURES	26
2.1. Instrumentation, Anemometers	26
2.2. Survey of the Test Volume.....	30
2.3. Pointwise Measurements.....	33
2.4. Instrumentation, Test Turbine	35
3. WIND GENERATION SYSTEM.....	39
3.1. Wind Generation System Configuration.....	41
3.2. Results and Discussion.....	44

4. COMPARISON OF WIND GENERATOR AND WIND TUNNEL BEHAVIOR AND THE IMPACT OF NEARBY WALLS ON WIND GENERATOR PERFORMANCE	57
4.1 Wind Tunnel Configuration	58
4.2 Comparison of Wind Generator to Wind Tunnel Flow.....	59
4.3 Turbine Performance Comparison from Wind Generator to Wind Tunnel Configuration.....	64
4.4 Facility Wall Effect.....	69
4.5 Active Recirculation	73
5. CONCLUDING REMARKS.....	77
REFERENCES.....	81
APPENDIX A FLOW SEPARATION.....	86
APPENDIX B UNCERTAINTY ANALYSIS	89
BIOGRAPHY OF THE AUTHOR.....	91

LIST OF FIGURES

Figure 1.1. Floating platform concepts for offshore wind turbines	3
Figure 1.2. Open-circuit wind tunnel, downstream power source	12
Figure 1.3. Open-circuit blower type tunnel, upstream power source	12
Figure 1.4. Closed-circuit tunnel showing changes in wind speeds throughout.....	13
Figure 1.5. Closed-circuit tunnel with an open jet test section (air flow is clockwise as pictured).....	14
Figure 1.6. Evolution of shear zone surrounding the test section	15
Figure 2.1. Hot wire and acoustic anemometer location.....	27
Figure 2.2. Hot wire anemometer element with an active sensor length of 1.25mm.....	27
Figure 2.3. Coordinate system used to describe test jet.....	29
Figure 2.4. Colored lines indicate the paths taken by the anemometers with respect to a projection of the nozzle (black line) to create one planar survey	31
Figure 2.5. Location of planar surveys throughout the test section.....	32
Figure 2.6. Location of planar surveys throughout the test section with a test turbine located 1.0 m from the nozzle	33
Figure 2.7. Location of stationary data collection sites	34
Figure 2.8. Test Horizontal-axis Wind Turbine Used in Trials.....	36
Figure 3.1. The different sections of the one-third scale wind-tunnel in an open jet, closed-circuit configuration.....	41

Figure 3.2. The one-third scale wind generation system tested investigated in this chapter in an open jet, open-circuit configuration	42
Figure 3.3. The wind generator fan arrangement and nozzle are shown.....	43
Figure 3.4. A sample of the turbulence strength calculation is shown for a flow of 5m/s at the midsection.....	44
Figure 3.5. Flow field 0.5 m from the nozzle at 5 m/s using one screen.....	46
Figure 3.6. Flow field 0.5 m from the nozzle at 5 m/s using two screens.....	46
Figure 3.7. Flow field 0.5 m from the nozzle at 5 m/s using three screens	46
Figure 3.8. Flow field at 1.0 m from the nozzle using three screens with a 5m/s flow at the center point	48
Figure 3.9. Flow field at 1.5 m from the nozzle using three screens with a 5m/s flow at the center point	48
Figure 3.10. Flow field at 2.0 m from the nozzle using three screens with a 5m/s flow at the center point.....	48
Figure 3.11. Flow field with fan diffusers 0.5 m from the nozzle at 5 m/s using three screens	49
Figure 3.12. Flow field at 0.5 m from the nozzle using three screens with a 4 m/s flow at the center point (no turbine)	50
Figure 3.13. Flow field at 1.0 m from the nozzle using three screens with a 4m/s flow at the center point (no turbine)	51
Figure 3.14. Flow field at 1.5 m from the nozzle using three screens with a 4m/s flow at the center point (no turbine)	51

Figure 3.15. Flow field at 2.0 m from the nozzle using three screens with a 4m/s flow at the center point (no turbine)	51
Figure 3.16. Flow field at 0.5 meters from the nozzle using three screens with a 4m/s flow at the center point (with turbine).....	53
Figure 3.17. Flow field at 0.75 m from the nozzle using three screens with a 4m/s flow at the center point (with turbine)	53
Figure 3.18. Flow field at 1.25 m from the nozzle using three screens with a 4m/s flow at the center point (with turbine)	53
Figure 3.19. Flow field at 1.5 m from the nozzle using three screens with a 4m/s flow at the center point (with turbine)	54
Figure 3.20. Flow field at 2.0 m from the nozzle using three screens with a 4m/s flow at the center point (with turbine)	54
Figure 3.21. Mean velocity at the hub height location without the turbine	55
Figure 3.22. Mean velocity at the hub height location with the turbine	55
Figure 4.1. Wind tunnel shown in open jet, closed-circuit configuration	58
Figure 4.2. Velocity and turbulence profile 0.5 meters from nozzle of wind generator “open-circuit”	60
Figure 4.3. Velocity and turbulence profile 0.5 meters from nozzle of wind tunnel “closed-circuit”	60
Figure 4.4. Flow velocity along the vertical centerline for both configurations	61

Figure 4.5.a. Turbulence intensities for a mid-elevation tunnel transect 0.5 meters in front of the nozzle.....	62
Figure 4.5.b. Velocities for a mid-elevation tunnel transect 0.5 meters in front of the nozzle at 5 m/s.....	62
Figure 4.6. Velocity and turbulence 0.5 m behind a turbine placed 1m from the nozzle of the wind generator operating at 4 m/s	64
Figure 4.7. Velocity and turbulence 0.5 m behind a turbine placed 1m from the nozzle of the wind tunnel operating at 4m/s.....	65
Figure 4.8. Power coefficients for a test turbine operating in both wind systems at various wind speeds	66
Figure 4.9. Thrust coefficients for a test turbine operating in both wind systems at various wind speeds	66
Figure 4.10. Flow at mid elevation in front of test turbine in both wind systems	68
Figure 4.11. Flow at mid elevation behind test turbine in both wind systems	68
Figure 4.12. Test configuration for the wall sensitivity study.....	70
Figure 4.13. Power and thrust coefficients of a test turbine in response to the proximity of a wall perpendicular to the flow, downstream of the turbine	72
Figure 4.14. Normalized power coefficients of a test in response to the proximity of a wall perpendicular to the flow, downstream of the turbine	72

Figure 4.15. Test configuration for the active recirculation effectiveness study.....	73
Figure 4.16. Power and thrust coefficients of a test turbine in response to varying power supplied to the active bank of fans	75
Figure 4.17. Normalized power and thrust coefficients of a test turbine in response to varying power supplied to an active bank of fans	75
Figure A.1. Behavior of streamers installed on the vertical walls of the diffuser as viewed along the downstream direction	87
Figure A.2. Visualization of separation within the return section of the wind tunnel.....	88

CHAPTER 1

FLOATING OFFSHORE WIND TURBINE DEVELOPMENT

This chapter will elucidate the current state of the art of floating offshore wind turbine (FOWT) development. From the motivations to advance this technology to the different configurations of floaters available to designers it will seek to explain the advancements that have already been made as well as the direction future work will take. Numerical codes critical to the design and analysis of FOWT development and the validation methods of these codes will be discussed. Empirical validation of numerical codes through physical modeling will highlight the considerations that must be made when testing scale models as well as the methods and procedures that researchers have already taken to produce experimental data. Representative experimental testing of a FOWT requires the accurate replication of both waves and wind conditions with the latter being the focus of this work. The fundamentals of wind tunnel design and various successful tunnel configurations will be discussed. Testing facilities, their past achievements, and their present capabilities will additionally be explored. In doing this, the shortcoming of early turbine tests will act as a guide for the design requirements of future, more capable testing facilities. The Harold Alfond W² Ocean Engineering Laboratory wind-wave facility constructed at the University of Maine is one such facility. The development of the wind generation system used in this facility will be investigated in various configurations with the resulting performance presented in subsequent chapters. These additional chapters will investigate and present the influences of facility wall effects to turbine and wind generator performance as well

as the effects of recirculation and other mitigation measures on turbine and wind generator performance.

1.1 Motivations

The next step in the development of wind-based renewable energy is in the field of floating offshore wind energy systems [1]. Pursuit of higher energy content wind resources is driving exploration further from shore into deeper water. In the United States some of the greatest offshore wind energy resources exist at locations where the water depth is often great regardless of proximity to shore [2]. It has been calculated that there is a consistent wind power density greater than 400 W/m^2 at 20-50+ miles offshore of the US northeast coast. At these potential wind energy sites the depth of water usually makes the use of fixed-bottom monopole or jacket foundations economically unfeasible. Floating offshore wind turbines and new technologies will need to be developed in order to make use of these sources of energy, and to make offshore wind farms cost competitive with their terrestrial counterparts.

1.2 FOWT Design and Analysis

To aid in research of offshore wind turbines, the National Renewable Energy Laboratory (NREL) has specified a 5 MW reference turbine [3]. This turbine is commonly looked towards as a model to be adapted for use in floating turbine research when seeking to expand knowledge in the field. The floater designs for

FOWTs can be classified into three main categories: tension-leg platform (TLP), spar-buoy and semisubmersible as seen in Figure 1.1 [4, 5]. Each of these floater designs has its benefits and shortcomings and is differentiated by how the interaction of their weight, buoyant force, and mooring line forces contribute to the stabilization of the platform. The tension leg platform uses tensioned mooring lines to partially submerge the platform below its natural floating equilibrium position. It is this tension that acts to right the platform when perturbed. TLP-based floating wind turbines are in various stages of testing and development with significant advances already made by such companies as Glosten Associates (PelaStar), IBERDROLA (TLPWIND), and GICON [6, 7].

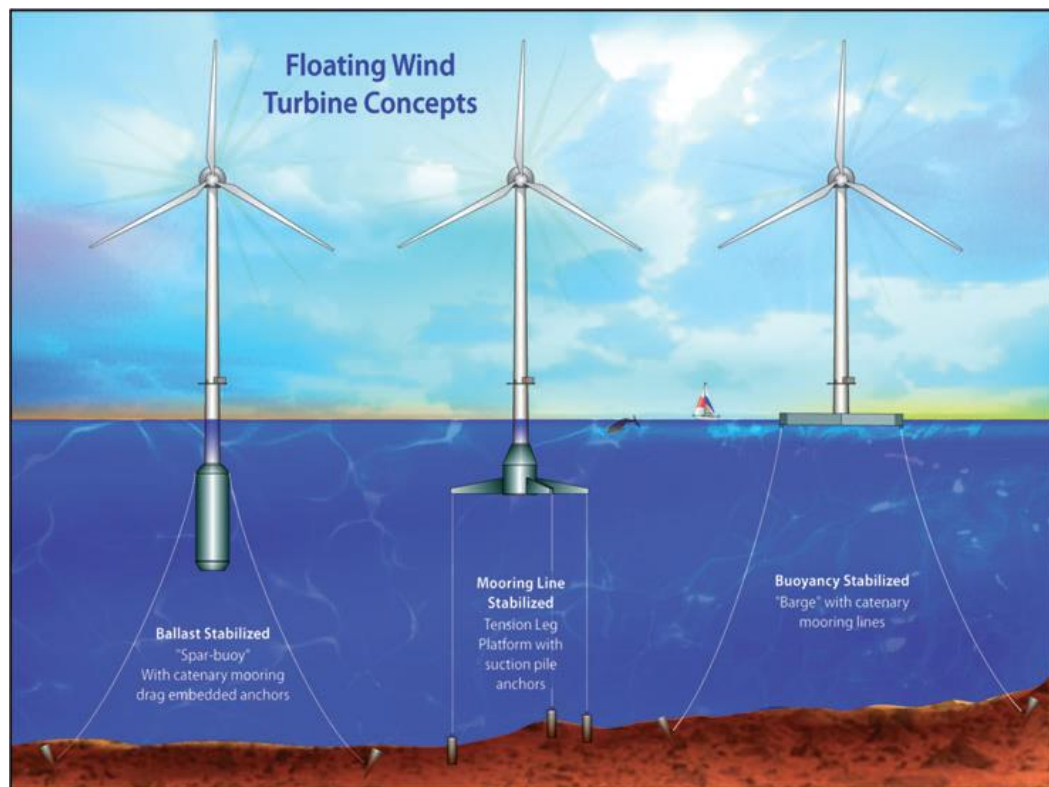


Figure 1.1. Floating platform concepts for offshore wind turbines [8].

The spar-buoy locates the center of gravity far below the center of flotation to create a righting moment when upset. In 2009 Statoil installed Hywind, the first commercial-scale FOWT in the world [9]. This 2.3 MW spar-buoy mounted turbine has functioned as a testing ground for research and has yielded data that will assist in their next endeavor of creating a 3-5 turbine wind farm. The Fukushima Forward project's second phase includes the deployment of two 7 MW turbines that will be integrated into their existing wind energy testing grounds [10]. One of these will be mounted on what is being called an advanced spar, or a spar-buoy that incorporates several heave plates. The SWAY floating wind turbine is a combination of a TLP and a spar buoy comprised of a floating tower that is submerged by a single tension leg and swivel [11]. The Sway FOWT foundation is designed to accommodate a 5-12 MW class downwind turbine. This last concept demonstrates the flexibility of design that a combination of these foundation types permits.

The semisubmersible platform uses a large footprint to distribute the buoyant force acting on the platform that results in a righting moment to stabilize the platform when upset. Semisubmersible variants range from early conceptual stages of development to full-scale deployment of power producing units. WindSea is a semisubmersible concept in the early stages of development [12]. Like many semisubmersibles WindSea uses a tri floater design; however this platform is intended to support three separate wind turbines instead of the usual one. WindSea has conducted scale model testing in wind, wave, and wind-wave

environments to validate performance and aid in full scale design. There are also several semisubmersible floating wind turbines in operation today as model demonstrators and in situ testing mechanisms. Principle Power has installed WindFloat, a full scale prototype, successfully off the coast of Portugal [13]. The University of Maine installed VoltturnUS, a 1/8-scale prototype of a 6 MW commercial design in 2014 off the coast of Maine [14]. This onsite testing allowed for the collection of data useful in determining the performance and survivability of a full scale turbine. Off the coast of Japan, the Fukushima Forward project has installed a 2 MW turbine in the first phase of an ongoing project to establish the business model for a FOWT farm. The second phase of the Fukushima Forward project will include the deployment and integration of a 7 MW turbine mounted on a V-Shaped semisubmersible into this wind farm [15].

When a turbine is placed on a floating foundation with six degrees of freedom the coupled effects of the wind and wave environments on the machine greatly increase the complexity of model simulation and analysis. For land based turbines, numerical codes have been created to run independently and model the response and behavior of horizontal-axis wind turbines (HAWTs) to specific influencing forces. These stand-alone codes can be integrated to allow fully coupled aero-servo-elastic modeling of land based turbines. These codes require the consideration of aerodynamic loads, gravitational loads, inertial loads, reactionary torques, gyroscopic effects, control forces and structural dynamics. A floating turbine foundation greatly increases the complexity of system modeling in

that it becomes subject to the reaction forces resulting from the wind loading of the turbine itself. Any resulting motion of the turbine will change its performance and alter the reaction forces. For example a turbine that pitches back and forth will have different inflow velocities as it rocks in one direction as compared to the other, resulting in varying turbine thrust and performance. To accommodate the additional dynamics pertinent to offshore installations, additional numerical codes have been developed to model incident waves, sea currents, hydrodynamics, mooring lines, and foundation dynamics of the support structure (see Figure 1). A complete fully coupled numerical model of a floating wind turbine would need to incorporate all of these loadings successfully [5, 16]. Numerical codes are a critical tool in the development and analysis of new FOWT technology as they permit prediction of the coupled dynamic response of the machine, as well as the fatigue and extreme loads of the system. These codes enable developers to arrive at safe, optimized, and robust FOWT designs. The high complexity and sophistication of these simulation codes underscores the need to verify and validate their accuracy [17].

1.3 Numerical Codes and the Need for Experimental Validation

Numerical codes can be a powerful design tool for FOWT technology as long as they can accurately model real world behaviors. The accuracy of numerical codes can be verified by comparing their results to other numerical codes or to empirical data gathered from scale model tests. Obtaining model-scale test data presents many advantages over full-scale data as it can be created in a controlled

laboratory setting with far less cost and risk than an instrumented, field-deployed prototype. As such, wind tunnel and wave basin testing are well suited for generating data for validating numerical code predictions. In addition to validating computational models, scale testing can yield experimental data that can be used as input variables to subsequent computational analysis. Numerical modeling and scale testing both have their place in investigating new offshore wind technologies, cost optimization, and survivability studies [15, 18, 19].

Numerical codes to model certain behaviors of FOWTs are commonly available. The US Department of Energy's National Renewable Energy Laboratory (NREL) has sponsored the development, verification, and validation of several successful codes including; FAST, AeroDyn and MSC.ADAMS® (Automatic Dynamic Analysis of Mechanical Systems). FAST-OrcaFlex, FAST-Charm3D, and Simo/Riflex are combinations of coupled numerical codes that can interface with standard wind turbine simulation tools, handle hydrodynamic modeling, and are gaining acceptance in the field of FOWT. These numerical codes are just a few of the ever growing number of programs available to FOWT developers. A more comprehensive list of the available codes is provided in the OC4 publication discussed in the next section [17, 20-22].

Code-to-code verification can be accomplished by such efforts as the Offshore Code Comparison Collaboration, Continuation (OC4) project established by the International Energy Agency (IEA) Wind tasks. This effort was performed

through a technical exchange amongst a group of international participants from universities, research institutions, and industry around the world. In an effort such as this, an offshore wind system design is identified and the information needed to model the system is developed and shared with the project partners. The participants build a numerical model of the given design with their respective modeling tools and run the prescribed load cases. The simulated response behavior (loads/motions) is then compared among the various codes at multiple points throughout the system. This allows mistakes in the modeling implementation or simulation settings to be identified, shows differences in the resulting loads/motions based on the modeling approach, and spurs discussion about the differences between and applicability of the various modeling theories. This procedure was repeated for multiple offshore wind system designs. Code-to-code comparisons such as this effort have been extremely useful in showing the influence of different modeling approaches on the simulated response of an offshore wind system. However, code-to-code comparisons can only identify differences; they do not determine which solution is the most accurate [17].

To determine the accuracy of numerical codes and assess their validity as an offshore wind modeling tool, there needs to be agreement between code simulation results and experimental results. The Offshore Code Comparison Collaboration Continuation, with Correlation project (OC5) is intended to continue where OC4 left off and validate offshore wind modeling tools through the comparison of simulated responses to physical response data from actual

measurements. OC5 will run from 2014 through 2018 with the first phase focused on examining the hydrodynamic loads on fixed cylinders tested under regular and irregular wave conditions at MARINTEK. A wind turbine is omitted in these tests to isolate and examine only the hydrodynamic loads, before moving on to the complexity of coupled wind/wave loads and dynamic system response. Phase II will include more complex geometry and coupling with turbine aerodynamic loads and control, focusing on the validation of a floating offshore wind system tested in a laboratory environment [23]. Subsequent phases will examine three structures using data from both floating and fixed-bottom systems, and from both scaled tank testing and full-scale, open-ocean testing. In extrapolating the efforts of OC4 and OC5 it becomes apparent that the industry will require new adept wind-wave test facilities to produce empirical data for validation of its offshore floating wind numerical tools.

1.4 Experimental Methods

In addition to numerical code validation, other motivations exist that drive the need for experimental testing of scale FOWT models. Often times physical testing is the best means for technological development in this field. For example, conceptual validation and proof of concept is better suited to physical models. This is especially true for uncommon systems or situations that may be difficult to simulate such as vertical-axis wind turbines, multi-turbine arrangements, unique installations, or deployment operations. Additionally, offshore turbines must be able to withstand extreme environmental conditions which can be simulated

experimentally through wind-wave testing. Lastly, data collection from physical testing will continue to expand the growing collective knowledge in this field which is likely to produce new ideas and concepts in the offshore wind energy sector.

Experimental testing of scale FOWT models has been carried out in a variety of different ways. A look at past testing campaigns shows the variety of methods experimenters have used to test scale models. The next section will look more closely at some of the procedures used to test FOWT models. These methods vary greatly from applying wind loads to floating models, applying hydrodynamic loads to aerodynamic models, and subjecting models to simulated wind-wave environments.

When a suitable wind-wave testing environment has not been available certain studies have tried instead to apply the generation of a wind load on a floating model instead of a wind field [24]. This is accomplished by mounting a single variable speed controllable ducted fan to the floating structure itself with the intent of simulating the forces experienced by a turbine in a real wind field with the reaction forces experienced by the mounted fan. However, with fans on the model, it is difficult to have the correct point of wind load application; this results in incorrect aerodynamic moments. Furthermore, wind is not only a load, but also provides damping and self-excitation including vortex-induced vibrations, which are realistically modeled with a real wind field only [25, 26]. Alternatively, others have mimicked the aerodynamic and hydrodynamic coupling of floating offshore

wind energy systems in scale tests by operating a model wind turbine that is fixed to an actuating base to simulate the motions of a floating platform while the turbine operates in a test wind flow [27]. Isolation and independent simulation of different loadings may have its worth in validating independent numerical packages but it fails to comprehensively test the coupled behavior of a scale model in a simulated wind-wave environment. For the purposes of conducting such a comprehensive experiment, a testing facility must be able to generate a wind field that can be applied to a model located in a wave basin. Section 1.6 will introduce and discuss a few facilities that are capable of generating such an environment today.

1.5 Wind Tunnel Design

The earliest wind tunnels were also among the simplest. The name given to these tunnels, open-circuit (Figures 1.2 and 1.3), describes how the air is used only once within the tunnel. Fresh air would continually enter one side of the tunnel and exit the other. In an open-circuit tunnel the power source can be located downstream of the test section (where experimental testing occurs) as in Figure 1.2 or upstream of the test section as in the blower type of tunnel shown in Figure 1.3. In the latter case, the air entering the test section needs to be conditioned properly to correct for the turbulence and swirl resulting from the power source. An advantage of this type of tunnel compared to other configurations is that tunnel testing and any resulting disturbance to flow in the test section is not recirculated preventing possible compromise of the tunnel's performance. Open-circuit tunnels

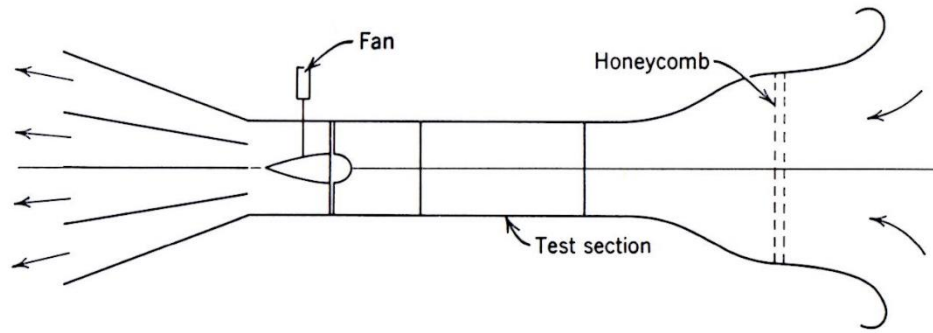


Figure 1.2. Open-circuit wind tunnel, downstream power source [28].

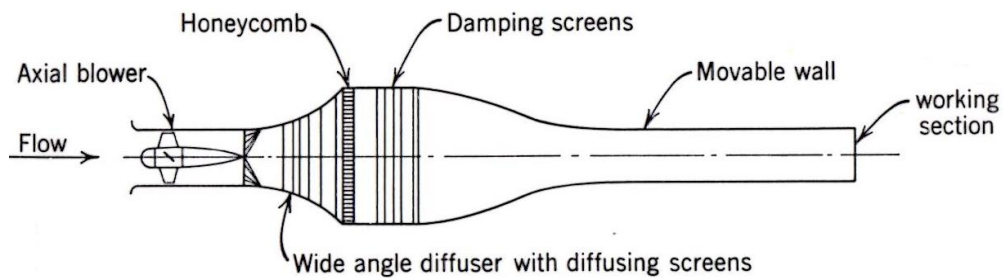


Figure 1.3. Open-circuit blower type tunnel, upstream power source [28].

routinely vented to the outside of the building they are housed in with fresh air entering one side of the facility and exiting the other.

When open to a vast and still environment such as the atmosphere with no wind, open-circuit tunnels perform consistently well. These external conditions, however, are uncontrollable leaving this tunnel susceptible to changes in performance due to natural occurrences like wind gusts. Enclosing an open-circuit tunnel entirely within a large building eliminates the concerns of interference due to wind and weather events while introducing a new potentially interfering effect; the building itself. When enclosed in a building an open-circuit tunnel requires enough free room around it so that the quality of air entering the tunnel is not affected significantly [29]. An alternative configuration of wind tunnel, the closed-

circuit tunnel (Figure 1.4), is intended to improve upon the open-circuit variety. The closed-circuit tunnel has the advantage of being able to control the return flow to the tunnel providing uniform, gust free, and sometimes temperature controlled air back into the system [28].

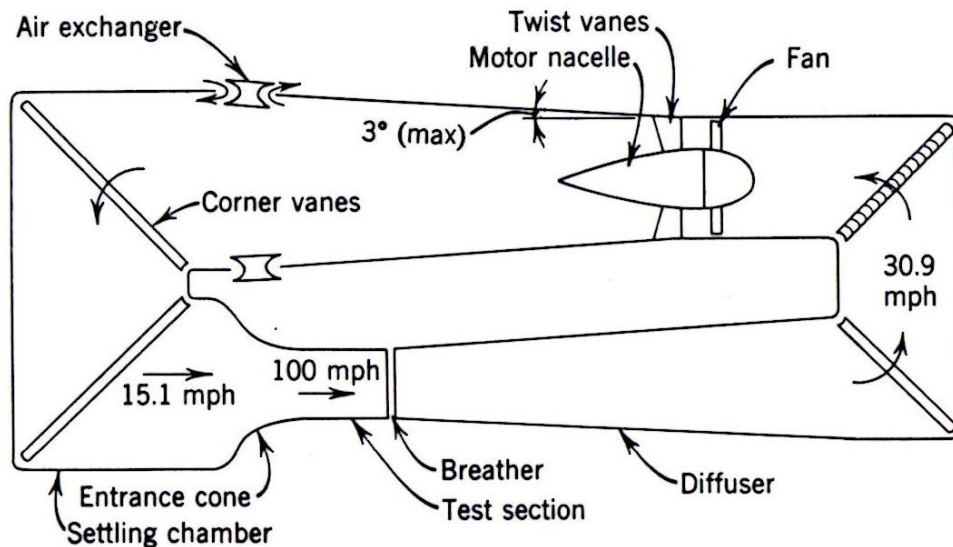


Figure 1.4. Closed-circuit tunnel showing changes in wind speeds throughout [28].

When building an enclosed test facility it is likely that financial pressure will push for larger wind tunnels within smaller facilities driving down the physical clearances between the two. If an open-circuit tunnel is desired, the air used in the tunnel is drawn from and returned to the building repeatedly. In this particular arrangement, if the clearance between the tunnel and the building becomes too small the open-circuit tunnel essentially become a closed-circuit tunnel with a poorly designed return leg. Moreover, the parameters of this impromptu “closed-circuit” configuration may change with the repositioning of the tunnel within the building. However, with careful consideration it has been shown that it is possible

to achieve high performance from an open-circuit tunnel inside of a building, thus saving space, weight, and the associated 60-100% increase in construction costs usually associated with closed-circuit configurations [28, 29]. The test section in either type of wind tunnel can be built with either an open test section as shown in Figure 1.5 or a closed test section as shown in Figures 1.2-1.4.

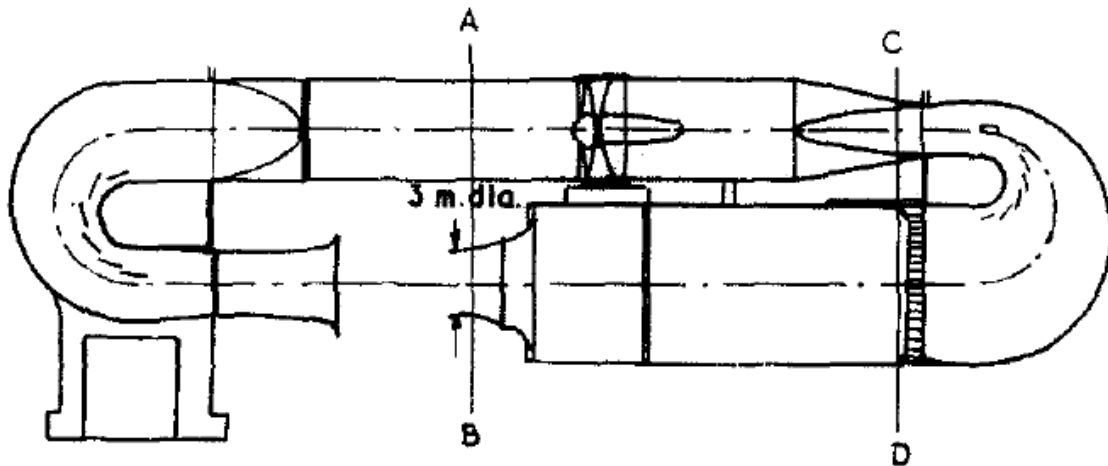


Figure 1.5. Closed-circuit tunnel with an open jet test section (air flow is clockwise as pictured) [30].

The main benefit of an open jet variant is access to the model and is a must for a tunnel intended to test scale FOWT models that are floating in a wave basin. A small draw back to the open jet variation is that it consumes more power compared to the closed jet tunnel as stagnant air surrounding the test section is entrained into the flow by turbulent mixing at the perimeter of the jet and momentum is lost in the compensating outflow as the jet enters the collector [30]. This turbulent mixing along the perimeter makes up a shear zone (Figure 1.6) that

defines the bounds of the testable area in an open jet tunnel configuration, it can be seen to grow as distance downstream from the nozzle increases.

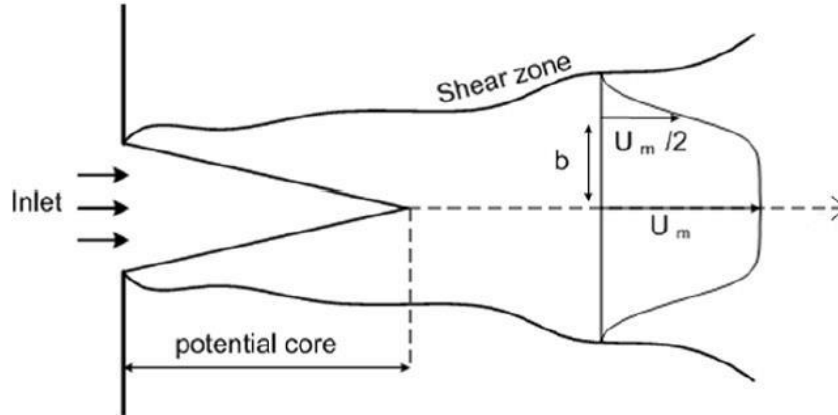


Figure 1.6. Evolution of shear zone surrounding the test section [31].

The open jet tunnel variation can also be applied to either of the open-circuit configurations shown in Figures 1.2 and 1.3. Of the two open-circuit configurations shown above, an open jet variation is more easily implemented with the blower type tunnel. When an open jet is used with a downstream drive open-circuit tunnel, most of the air enters the tunnel at the end of the test section at the collector with little stream across the actual test section [28]. One advantage of the open jet over the closed jet test is that the closed jet confines the flow of air in the test section and does not allow it to expand as it encounters the model being tested. When testing a wind turbine there is naturally some blockage effect in front of the model as the incoming air slows down when it encounters the turbine. This results in some of the flow being redirected around the turbine which is easily accommodated in an open jet test section and discouraged in a closed jet test

section. Therefore, an open jet test section is better suited for testing wind turbines as it more closely approximates the infinite flow field experienced in real wind conditions.

In section 1.7 it will be seen that current facilities with FOWT wind-wave testing capabilities have arrived at the construction of an open jet, open-circuit, blower type wind tunnel. The open jet allows access and accommodation of floating models, the open-circuit arrangement keeps cost, weight, and ease of construction reasonable, while the blower type ensures proper flow across the test section. Each of these motivations for this type of tunnel also has its own cautionary measure that should be followed. The use of an open jet test section requires additional power and surrounds the test area with a highly turbulent shear zone. The open-circuit configuration needs special consideration to ensure that interaction with the structure of the building does not impact the performance of the wind tunnel. Lastly the blower type of arrangement will require special conditioning of the flow to remove turbulence created by the fans.

When testing wind turbines, quality wind is generally considered to be highly uniform throughout the test area with low turbulent intensity and a mean flow equivalent to the scaled wind velocities the model must experience. For example, a recent target set for performance specifications for the wind tunnel being built for the University of Maine calls for a spatial variation of 5% or less, turbulence intensity less than 4%, and wind speeds up to scale hurricane speeds [32]. The

methods for measuring and computing these values will be covered in the second chapter of this work. Wind tunnels generally employ the same components; their type, placement, and combination allow for tuning and optimization of a wind tunnel in pursuit of high quality wind generation. Most tunnels have a contraction before the test section. As the velocity of the air passing through the contraction increases, any velocity variations become a smaller fraction of the average velocity, a common way to decrease turbulence intensity. Additionally, the lower velocity of the air prior to the contraction reduces the power requirements of the fans. It is usual that the section immediately before the contraction has the largest cross section and thus the lowest velocities. This settling chamber provides an opportunity to condition the flow at lower speeds using honeycomb grid and mesh screens. The honeycomb acts to reduce irregularities in flow direction reducing turbulent strength. [30]. Screens increase flow uniformity by imposing a static pressure drop proportional to the velocity squared. A pressure drop coefficient of 2 will remove nearly all variation in longitudinal mean velocity reducing turbulent strength and turbulence intensity in the whole flow field [33]. In the section that follows, a closer look will be had at current wind-wave facilities, the steps they have taken to generate high quality wind, and the performance specifications of their current wind generating capabilities.

1.6 Testing Facilities and Accomplishments

Numerous facilities throughout the world possess a wind tunnel and a wave basin as a testing ground for scale FOWT models. Organizations such as the US

Naval Surface Warfare Center, Texas A&M, University of Iowa, Offshore Model Basin, Oceanic, Marintek, Maritime Research Institute Netherlands (MARIN), Oceanide, Ecole Centrale de Nantes, LabOceano, and the SSPA Maritime Dynamics Laboratory all currently offer a wave basin with a minimum depth of 3 meters and some level of wind generation capability. The 2011-2012 testing campaign by the University of Maine at MARIN highlights the needs and requirements of future testing facilities for FOWT development. In these tests, the three different floating variants of the 1/50th scale NREL 5 MW reference turbine were placed in a wind-wave basin. These tests required that the turbine be exposed to swirl free inflow at a turbulence intensity of about 5% as well as the ability to produce simultaneous stochastic wind and waves in addition to multidirectional sea conditions [34]. These testing requirements are driving the industry to continuously improve the performance of wave basin-specific wind tunnels available to the research community.

The DeepWind exploratory study involving an offshore floating vertical-axis wind turbine, demonstrates MARIN's attention to quality wind production [35]. These particular model tests were conducted to calibrate and validate the developed simulation codes within the project and to determine the response of the floating turbine. Considering the importance of the coupling between the aerodynamic and hydrodynamic behavior of floating wind turbines, the modelling and documentation of the wind field in MARIN's Offshore Basin during the model tests is of great importance. At the time of these tests existing wind generation

systems were not sufficient for accurate wind turbine testing, with some wind created by banks of box fans. MARIN responded by developing a local wind field produced by a square bed of 25 (5 by 5) wind fans with guides and stators close to the turbine. By controlling the fan RPMs in the different rows, the vertical profile of the wind could be controlled, and an approximation of wind shear could be simulated. This wind generator was designed with the help of computational fluid dynamic (CFD) software and tested outside the basin to determine and limit turbulence levels [36]. More recently MARIN has developed an improved wind generation system to meet the need of today's experimental tests. It was originally developed for the DeepCwind Consortium, a partnership of approximately 30 members around the country desiring to develop deep water offshore wind technology, and has since been used in several other testing campaigns. The high quality wind environments, unique to these tests, were realized in the offshore basin via a novel wind machine that exhibits negligible swirl and an average turbulence of less than 5% intensity in the flow field. This was accomplished with a bank of 35 fans, a honeycomb front plate to reduce swirl, and a nozzle to reduce turbulence [15]. The output area of the nozzle covered the entire wind turbine rotor through its expected range of motion. With all of the benefits this wind generation system there were still some drawbacks. The bank of fans needed to be placed high enough as to not interact with the water, resulting in a decreased wind speed on the lower portion of the rotor. This deficiency in flow was mitigated with an approximately 2 degree downward tilt, improving the wind speeds at the bottom of the rotor, but at the expense of introducing a vertical component to the wind

velocity. The development of this wind generation system yielded valuable information into the interaction of the wind generator with the building it is housed in. The most observable effect of the facility walls on the performance of the wind system is that the fans require special attention due to the recirculation of the wind field in the basin and the variation of the wind speed with the distance from the fans [37]. The effects of facility walls on the performance of wind generation systems will be discussed in greater detail in chapter three of this work.

At Ecole Centrale de Nantes, efforts have been made as well to produce a wind generation system that meets the consumer's' needs. There a wind system has been developed that utilizes centrifugal fans instead of axial fans to avoid the generation of a twisted flow which introduces spatial inhomogeneity and high turbulence levels. Additional steps were taken to reduce turbulence, increase homogeneity, and improve the quality of flow based on proven wind tunnel design with the inclusion of a screen and a honeycomb. Using the CFD package Fluent, the designers were able to visualize the average stream wise velocity behind the blow nozzle and anticipate a lack of speed in the center of the jet. This deficit was expected since the four circular elements do not carry the momentum of the fluid in the center of the flow despite the use of diffusers. To avoid the potential problems that may arise in the study of structures moving in the wind, like floating wind turbines, a convergent form was developed to homogenize the velocity profile. The improved wind generation system was qualified on the wave basin with a survey of the test area using a sonic anemometer to further demonstrate the

capabilities of a facility like this to model, produce, measure, and verify the quality of wind they are able to generate. The qualification process after the convergent form was installed showed a homogeneity of the average velocity in the test area that met the design requirements. The effectiveness of the convergent form was clearly demonstrated in the elimination of the expected deficit in the center of the jet. Additionally a turbulence level equal to 3% was measured at the center of the jet, which is very low for this type of installation. All these results prove the relevance of the artifices used to reduce turbulence and homogenize the flow as well as highlight the measures that a facility can take to produce, tune, measure, and assure high quality wind [38].

1.7 Test Flow Sensitivity

The same technologies used to assess the quality of wind generation systems have applications in model turbine testing. Specifically, acoustic and hotwire anemometers can be used throughout the testing volume containing the turbine to yield information on the environment the model is exposed to as well as the model's effect on the environment. An example of such a survey can be found in the test set-up section in chapter two of this work. The ability to survey the inflow air the turbine ingests gives one the necessary information to insert tested wind environments into numerical models for the purposes of making fair comparisons in validation studies. Surveying the flow downstream from a model can also yield information on the effects of a scale model on its environment. Of particular interest is the development of a turbine's wake, which can be measured by surveying the

test flow in the shadow of a test model. This may be desired to substantiate CFD or other numerical code results, provide insight into turbine performance, as well as aid in the planning and layout of wind farms [39]. The implications for wind farm planning being that turbine performance can suffer when operating in the wakes of other turbines. As surveying improves, faster sampling rates, increased sensitivity, and higher resolution scanning of the test volume will yield information that will be increasingly more valuable in validating CFD results as discussed by de Ridder [40].

1.8 Development of Future Facilities

In addition to being able to generate quality wind, today's state of the art facilities must be able to operate in conjunction with a wave basin appropriately. When testing offshore floating wind energy devices the primary criteria of the testing facility becomes the accurate replication of winds and waves that exist in the open ocean. In a real ocean environment, waves and winds are not always collinear. To replicate this environment, wind and waves must be generated in various orientations to one another. This can be accomplished by changing either the wind or wave direction. The University of Maine has constructed the W^2 wind-wave facility to meet these testing needs at a 1/50th scale for 5 MW offshore floating wind turbines [41]. The novelty and relevance of this facility are attributed to its ability to generate wind and waves in various orientations as well as the increased size and wind capacity over past experimental efforts detailed in section 1.6.

The W² wind-wave facility will be able to generate complex sea states and accurately replicate any direction of wind flow relative to the motion of waves by rotating a wind generation system above a wave basin to various positions before testing floating structures. When rotating the wind generator within the facility the distance between the wind generator and the walls of the facility may vary significantly. In section 1.5, proximal building walls were linked to an adverse effect on the quality of wind produced in the test section of an open-circuit tunnel. Successful rotation of a similar wind generation system above the wave basin is contingent on the tunnel's ability to be insensitive to the different boundary conditions imposed by the building when rotated through different orientations. The degree to which changes in generator-building orientation will effect wind generation quality in this particular facility are unknown as of the beginning of this study. This work will include an investigation into the sensitivity of an open-jet, open-circuit tunnel (from this point forward referred to as the wind generation system or wind generator) to changes in its position as well as an exploration of possible mitigation measures. A closed-jet, closed-circuit wind tunnel (although insensitive to the interference of the building walls with changes in orientation) is not a viable option for this particular application since it would not accommodate a model floating in a wave basin. Additionally, the size of such a tunnel necessary to avoid any blockage effects that would affect the performance of a model wind turbine would be great. This larger wind tunnel would drive up construction costs as well as the additional costs of the resulting larger building, possibly rendering such a facility prohibitively expensive. Construction costs, wind tunnel size, and

the necessary building required to house this facility are limiting factors in scale model FOWT testing. An alternative configuration that may reduce the wind generator's sensitivity to change in tunnel-building orientation is the conversion of the wind generation system to an open-jet closed-circuit arrangement (from here on referred to as the wind tunnel). Albeit more costly to construct than the wind generation system, configurations similar to the wind tunnel have been shown in section 1.5 to eliminate the sensitivity to orientation within a facility.

In the chapters that follow a wind generation system and a wind tunnel will be investigated to explore how each design can impact wind generation capability within a closed building. Exploration of these configurations may also yield information regarding how a test turbine responds experimentally to what may be different wind environments. Any differences in turbine performance from one configuration to the other would be of use to any researcher who would like to consider the impacts of the testing facility on their experiment. Stemming from this work will be an investigation into the influence of building wall effects on the performance of a scaled wind turbine and the ability of different tunnel configurations and active recirculation to correct such an impact.

This work will have direct applications to the design and use of the W^2 wind-wave facility. The findings of this investigation should be considered in the design of the final wind generation system. The sensitivity of the wind generator and the wind tunnel to the influences of the facility walls is a subject of great importance to

the design and construction of this particular facility. Additionally, the building wall effects on wind generation quality and test turbine performance can be used to confirm experimental findings and shape testing procedures.

CHAPTER 2

EXPERIMENTAL TESTING PROCEDURES

Successful wind turbine experimentation requires high quality wind flow. Researchers in the field consider a testing area large enough to accommodate the models being tested, a uniform flow field, low turbulence, and sufficient scale wind speeds as the measure of a suitable testing environment. This chapter will look at how these metrics can be measured in the laboratory setting. Multiple tunnel configurations in various arrangements are explored in this work with a one-third scale prototype. The scaling methods used to accomplish this will be discussed in further detail in subsequent sections. Results of these efforts could then be scaled up for guidance in the design and operation of the full scale tunnel being built in the W^2 facility. In all trials, the data collected is either a survey of wind flow in a vacant test section at steady state, a survey of the test section while a turbine is operating at steady state, or data pertaining to the performance of a turbine.

2.1 Instrumentation, Anemometers

Flow data in the test section was collected using an acoustic and a hot wire anemometer. The acoustic anemometer used is a R.M. Young Model 81000 (Figure 2.1) and it measures the mean velocity of the volume of air located in the middle of the instrument. This device measures the three-dimensional velocity field, collecting the mean speed as well as the direction of the wind in three

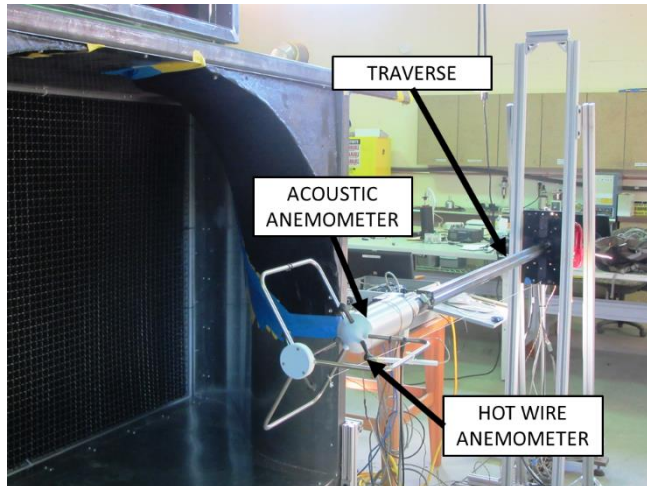


Figure 2.1. Hot wire and acoustic anemometer location.

dimensional space. This device can detect flows up to 40 m/s with an accuracy of ± 0.05 m/s. Data was collected from this device at a rate of 32 Hz. This acoustic anemometer functions by using three pairs of ultrasonic transducers oriented orthogonally to each other to determine the speed of sound in the volume being tested; in doing so the magnitude and direction of the fluid flow is revealed. The hot wire anemometer used is a Dantec Dynamics 55P01 wire probe anemometer (Figure 2.2) that measures flow speed at a sample rate of 5 kHz. This high sample rate allows the user to analyze rapid changes in air speed to determine the

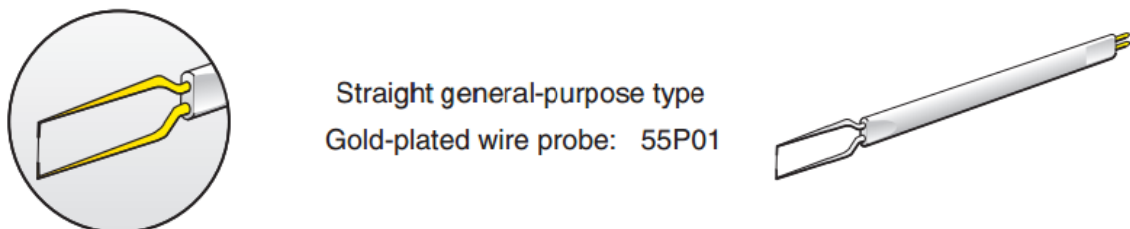


Figure 2.2. Hot wire anemometer element with an active sensor length of 1.25mm [42].

turbulent strength and turbulence intensity of the flow at the location of the wire. A hot wire probe is a type of constant temperature anemometer. The small wire element of the probe is essentially a resistance heater that is placed into the stream of air to be tested. The device functions by monitoring the current required to maintain a constant temperature in the element. In still air there is little convective heat transfer and therefore little current required to maintain its temperature. Air flow along the length of the wire does not offer a great deal of forced convective cooling, however flow in any other direction will have some component of velocity perpendicular to the wire element resulting in convective heat loss. By nature of its function, this type of anemometer is only able to collect information on the speed of flow in a plane that is perpendicular to the wire element. More complex and expensive hotwire probes can use multiple elements to determine information on the direction of flow. This hot wire probe was mounted with the element oriented vertically to be most sensitive to turbulence intensity within the horizontal plane where the nozzle contraction is the greatest and therefore the highest amounts of velocity fluctuation are anticipated. To determine the turbulence intensity in the test area the data sampled at 5 kHz by the hot wire anemometer is filtered to 2 kHz, to match the sample rate of the data acquisition system. The turbulence intensity is then calculated for a particular point using 400 neighboring data points with equations 2-4.

Turbulent flow is decomposed into a mean and time varying turbulent component:

$$u(t) = \bar{u} + u'(t) \quad (1)$$

$$v(t) = \bar{v} + v'(t)$$

$$w(t) = \bar{w} + w'(t)$$

$$U(t) = (u(t)^2 + v(t)^2 + w(t)^2)^{1/2}$$

where $u(t)$, $v(t)$, $w(t)$ are the component flow measurements, $U(t)$ is the combined flow measurement, \bar{u} , \bar{v} , \bar{w} , are the mean components of the flow and $u'(t)$, $v'(t)$, $w'(t)$, are the turbulent components in the x , y and z coordinates (Figure 2.3), respectively.

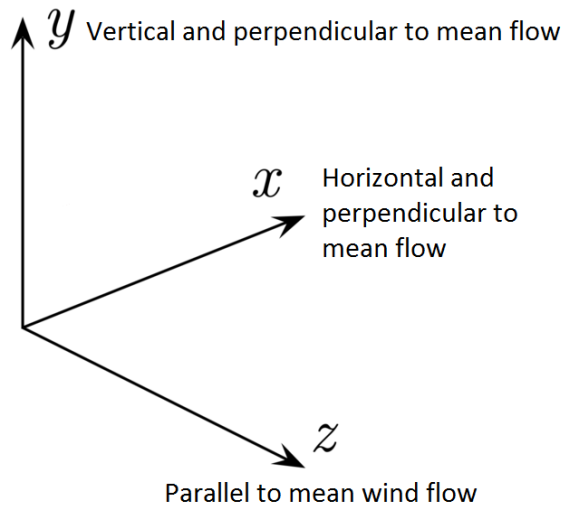


Figure 2.3. Coordinate system used to describe test jet.

The turbulent strength, u_{rms} , and turbulent intensity, $T.I.$, are then calculated as follows, where \bar{U} is the mean flow at the same location. It should be noted that \bar{w} is within 0.01% of \bar{U} as the net flow is predominantly in the z direction.

$$u_{rms} = \sqrt{\frac{1}{N} \sum_{i=1}^N (u'_i)^2} \quad (2)$$

$$\bar{U} = (\bar{u}^2 + \bar{v}^2 + \bar{w}^2)^{1/2} \quad (3)$$

$$T.I. = u_{rms}/\bar{U} \quad (4)$$

2.2 Survey of the Test Volume

The anemometers used collect information in a relatively small area. To get a truly representative picture of what is happening throughout the wind tunnel test section, data needs to be collected at many locations. This is accomplished by mounting both anemometers to the end of a traverse that moves slowly through the test section as data is collected. The hot wire probe is located 10 mm downstream from the center of the volume tested by the acoustic anemometer to ensure that the measurements are taken as close to the same location as possible (Figure 2.1.). The traverse moves the anemometers perpendicularly in and out of the test jet at ten different elevations each 160 mm apart from one another in a vertical plane that is parallel to the nozzle opening. The paths taken by the

anemometers extend from outside of the shear zone bordering the test area to beyond the centerline of the test section as shown in Figure 2.4.

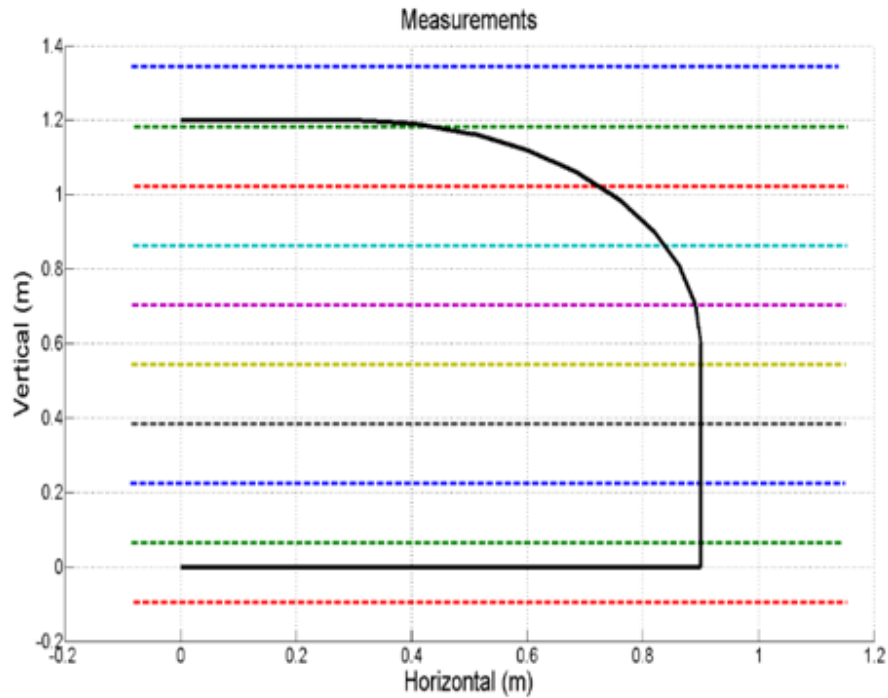


Figure 2.4. Colored lines indicate the paths taken by the anemometers with respect to a projection of the nozzle (black line) to create one planar survey.

Maps of the mean air velocity and turbulence intensity are produced using the data acquired from the survey of what amounts to 60% of the nozzle opening. In this study only the right hand side (when looking up stream) of the test section is surveyed in depth. Preliminary measurements taken manually with a hotwire probe confirmed equal flow on either side of the nozzle. Additionally, the wind generator utilizes screens and individually ducted fans (discussed further in section

3.1) to minimize the possibility of asymmetric flow. These precautionary measures and favorable manual measurements allowed this study to focus on the data gathered from only one side of the nozzle in response to different tunnel configurations and conditions. To understand how the flow field evolves as it travels through the vacant test section planar surveys are taken at 0.5, 1.0, 1.5, and 2.0 meters from the wind tunnel nozzle (unless otherwise noted) as shown in Figure 2.5.

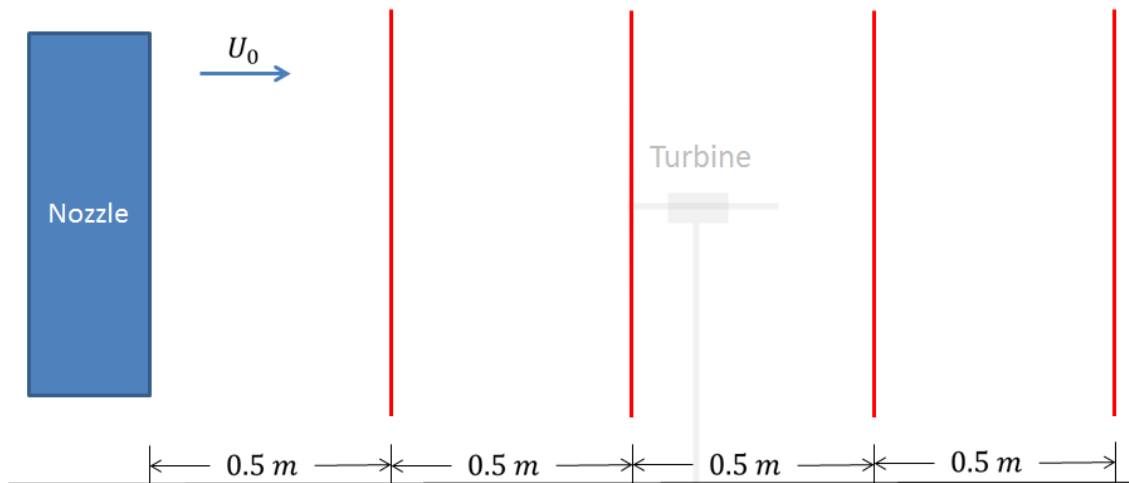


Figure 2.5. Location of planar surveys throughout the test section.

The same process is followed for surveying the flow in the presence of a test turbine with a slight change to the location of the planar surveys which are performed at 0.5, 0.75, 1.25, 1.5, and 2.0 meters due to turbine rotor being positioned at 1.0 meter (Figure 2.6). These contour plots could be analyzed in future efforts using cross correlation between sections to quantify change should more than a visual analysis be desired.

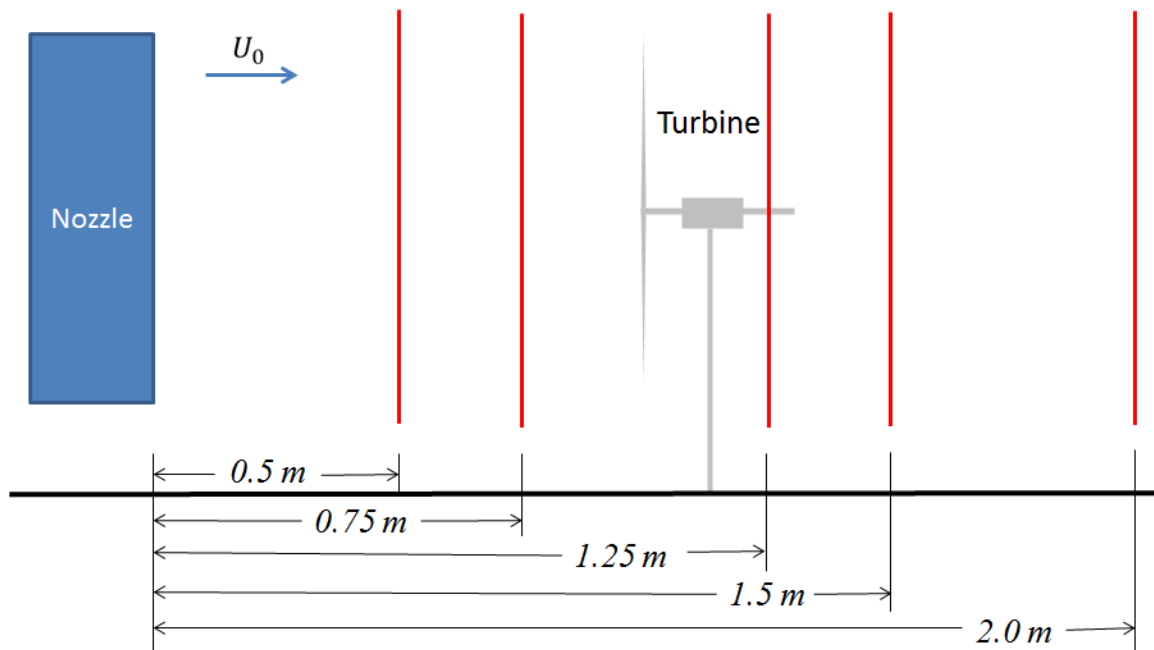


Figure 2.6. Location of planar surveys throughout the test section with a test turbine located 1.0 m from the nozzle.

2.3 Pointwise Measurements

An investigation has been made into the validity of the turbulence data collected in the previously described procedure. The traverse's speed of 38.8 mm/s or 0.78% of the maximum recorded wind velocity in the test volume was found to make any contributions to cross-flow components of air velocity negligible relative to the recorded flow speeds. However, with turbulence strength being the standard deviation of the fluctuations in flow velocity at a certain location over a period of time it could be argued that collecting flow data while moving the instrument is inappropriate for this task. The 400 data points used to calculate

turbulence values were collected over a relatively short 0.2 seconds, and in that time the instrument traveled 7.8 mm; a distance that is approximately 6 times larger than the sensor collecting the information and 230 times smaller than the width of the test area. To check the validity of turbulence data collected while moving the hot wire probe it was decided to measure turbulence values at fourteen different locations throughout the test section (Figure 2.7) over a thirty second period while keeping the hot wire probe stationary. It was found that turbulence data gathered while moving the hot wire probe were within 2% of the turbulence values measured while stationary. This exercise allowed for continued confidence in the turbulence data collected while moving the hot wire probe through the test section.

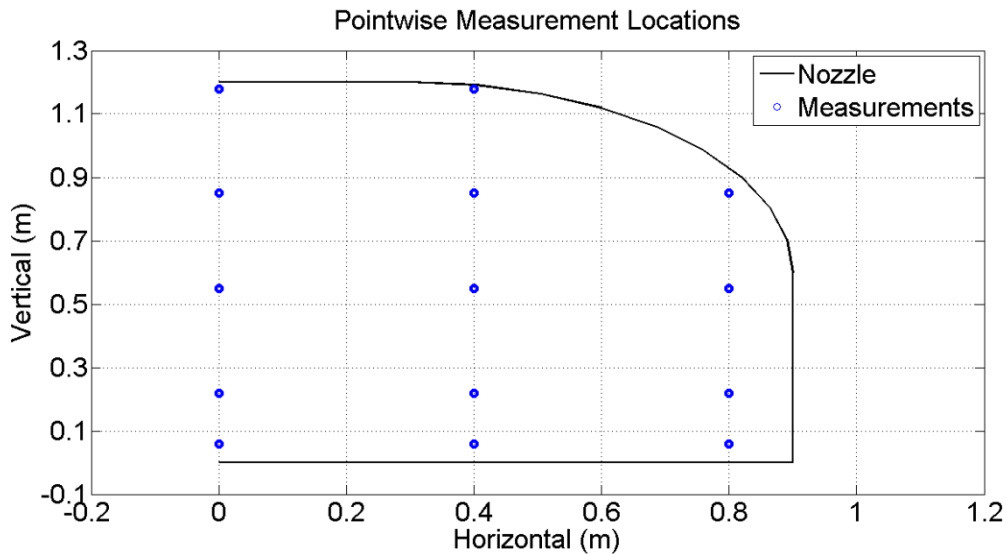


Figure 2.7. Location of stationary data collection sites.

An additional investigation was launched into the assumption that drove the decision to orient the hot wire probe vertically in the test section. Had this assumption been incorrect, any variability of flow in the vertical direction would have been unnoticed by the hot wire probe oriented parallel to these fluctuations.

Considering this, the hot wire probe was reoriented to be horizontal while still being parallel to the nozzle opening. The scanning data collection as well as the stationary data collection methods were repeated and compared to the vertically oriented probe data resulting in a decreased sensitivity to flow turbulence, reinforcing the earlier decision to mount the probe vertically.

2.4 Instrumentation, Test Turbine

Throughout these testing efforts a test turbine, shown in Figure 2.8, is used in various wind tunnel configurations and conditions as a data collection tool. The turbine used is essentially a geometrically scaled down version of the MARIN Stock Wind Turbine (MSWT). The MSWT is a 1/50th non-geometrically scaled performance matched model of the NREL 5MW reference turbine developed in response to the underperformance of a geometrically scaled model turbine. The poor performance of a Froude-scaled, geometrically similar model is due to the severe mismatch in Reynolds number between full scale and model scale. In creating the performance matched MSWT the mass and inertial properties of the turbine are geometrically scaled whereas the blade geometries must be modified to achieve appropriate drag, lift, thrust, and performance values at the lower Reynolds numbers associated with scaled tunnel test wind speeds [40, 43]. The non-dimensional power and thrust coefficients produced by this turbine are recorded to identify any differences in turbine output from one wind tunnel configuration to another.

The turbine's power coefficient, C_p , is calculated as follows:

$$C_p = \frac{P}{0.5\rho AU^3} = \frac{\bar{Q}\omega}{0.5\rho AU^3} \quad (5)$$

where P is the measured power extracted by the turbine, A is the area swept out by the turbine rotor, ρ is the density of the air, \bar{Q} is the average torque, ω is the angular velocity for the rotor and U is the mean velocity of air entering the turbine.

The turbine thrust coefficient, C_T , is calculated as:

$$C_T = \frac{T}{0.5\rho AU^2} \quad (6)$$

where T is the thrust experienced by the rotor in the direction of the incoming wind.

The scaled turbine used is a 1/130th scale (in relation to the 5 MW NREL turbine) three bladed HAWT with manually adjustable blade angles and a rotor radius of 0.486 meters. With the full-scale wind-wave basin intended to conduct



Figure 2.8. Test Horizontal-axis Wind Turbine Used in Trials.

1/50th scale turbine tests, a 1/150th scale turbine would be more appropriate for proving a one-third scale wind tunnel. The larger 1/130th scale turbine used in this campaign however demands even greater performance from the tunnel in terms of a larger operating area and higher quality flow at the nozzle extremities. At this scale, the turbine will demonstrate additional capacity within the tunnel for larger turbines. As a result, the wind-wave basin will continue to be able to provide 1/50th scale testing of turbines in excess of 5 MW as the industry continues to develop ever larger turbines. Previous experimentation with this scaled wind turbine has well documented results using a collective blade pitch angle of three degrees [40, 43], prompting the use of the same blade pitch angle throughout this work. The turbine has a six degree of freedom force and torque sensor directly below the nacelle that acquires the thrust experienced by the turbine, a torque sensor that links the turbine hub shaft to a motor shaft, and an encoder that measures angular position of the turbine for use in angular velocity calculations.

The turbine performance is calculated using a ramp test. The motor initially drives the acceleration of the non-self-starting turbine until the turbine begins to extract power from the wind flow, at which point the motor acts as a brake due to the rotor itself driving the acceleration. The torque from the ramp up is compared to the torque from the ramp down to eliminate any inertial factors involved in the angular acceleration. Additionally, the angular acceleration of the ramp test is kept low to allow the wake to stabilize and produce consistent performance close to that of steady state operation. The turbine's power coefficient is calculated using the

measured torque and associated angular speed using equation 5. The thrust coefficient is calculated using the acquired thrust from the six degree of freedom sensor using equation 6.

In addition to changes in turbine performance, it is desirable to gather information on any impact to the flow in the test section while the turbine is operating, such as turbine wake expansion, from one tunnel configuration to another. This is accomplished by conducting the survey of the flow in the test section flow, as described in section 2.3 and Figure 2.6, while operating the turbine at a steady state. In surveying the flow with a turbine, the angular speed of the rotor is adjusted relative to the mean wind speed selected for that particular test to maintain a blade tip speed ratio (TSR) of 7.6, where TSR is calculated as

$$TSR = \frac{\omega R}{U} \quad (7)$$

Non-dimensional rotor speed, as defined in equation 7, depends on the angular velocity of the turbine (ω), the mean velocity of air entering the turbine (U), and the radius of the turbine (R). The TSR chosen as the control variable is that which resulted in the maximum power coefficient in the initial testing of the scale turbine used. Through compilation of the collected data into maps of mean velocity and turbulence distribution at each cross section of the test jet, it is possible to visualize the effects of the turbine's presence on the test flow.

Chapter 3

WIND GENERATION SYSTEM

In pursuit of the larger objectives of this body of work, a wind generation system will be subjected to a variety of experimental procedures to establish baseline data that will be of value for comparison to the wind tunnel to be tested in the following chapter. This chapter will focus on the wind generator in just this configuration to characterize its wind generation capabilities. Additionally, these procedures allow the opportunity to tune the wind generator to improve the quality of wind it is able to generate through the installation and experimentation of screens in the settling chamber.

The design of the wind generation system to be used at the W^2 wind-wave basin is critical to the success of the testing facility. A one-third scale version of the wind generation system was constructed to gather baseline data for later comparison to its wind tunnel counterpart in an investigation into the performance sensitivity of different configurations to changes in position within a building. When scaling the findings of this study to the full scale wind generator, Froude scaling will be used for the global parameters of the wind generator [44], whereas elements such as honeycomb and screen will follow Reynold's scaling methods described in Bradshaw and Mehta [29], and Farell and Youssef [45]. The one-third scale wind generator's objectives are to test the system's sensitivity to building orientation, validate full-scale design, and produce a variety of scaled real-world wind conditions. The one-third scale wind generator has been designed to

generate steady state wind flow at 5 m/s as well as wind gusts. However, only steady state wind generation is presented in this work. At a one-third scale of the full size wind generator, Reynolds number scaling equates 5.0 m/s to a wind speed of 8.7m/s in the full-size tunnel (60m/s at full scale) meeting the specifications of the full-scale design. This specification will provide the wind generator with a measure of extra capacity to test the survivability of floating structures at 1/50th scale. More on the survivability of FOWT testing and the extreme wind loading of a parked rotor can be found from the 2011 DeepCwind testing campaign [46]. The investigation into the turbulence intensity within the test jet is conducted at the upper range of the wind generator's speed as this is where most of the turbulence issues are encountered. The majority of testing environments would not call for such severe winds. For comparison purposes, recent tests performed at MARIN were conducted at operating conditions of a floating turbine in real world scale winds of 21 m/s full scale (2.97 m/s at a 1/50th scale) [34].

In the work that follows a wind generation system will be characterized to map the available testing area, measuring the turbulence intensity as well as the homogeneity and velocity of flow throughout the testing area. Additionally the performance of a test turbine will be measured in this wind generation system. The information gathered in these procedures will serve as baseline data for use in comparison to alternate tunnel configurations detailed later in this body of work.

3.1 Wind Generation System Configuration

The wind tunnel in Figure 3.1 is constructed of three large sheet metal assemblies; the U-Return, the large horizontal diffuser, and one assembly that is composed of the fans, U-turn, settling chamber, and nozzle. This last assembly (seen in Figure 3.2) was constructed first and by itself functions as a wind generation unit. This wind generator is similar to the open jet, open-circuit tunnels introduced in chapter one with the slight difference of being bent back on itself through 180 degrees as opposed to the straight through design common to open-circuit tunnels. This wind generator is the focus of this chapter and its data may be referred to as “open-circuit” in figures throughout this body of work.

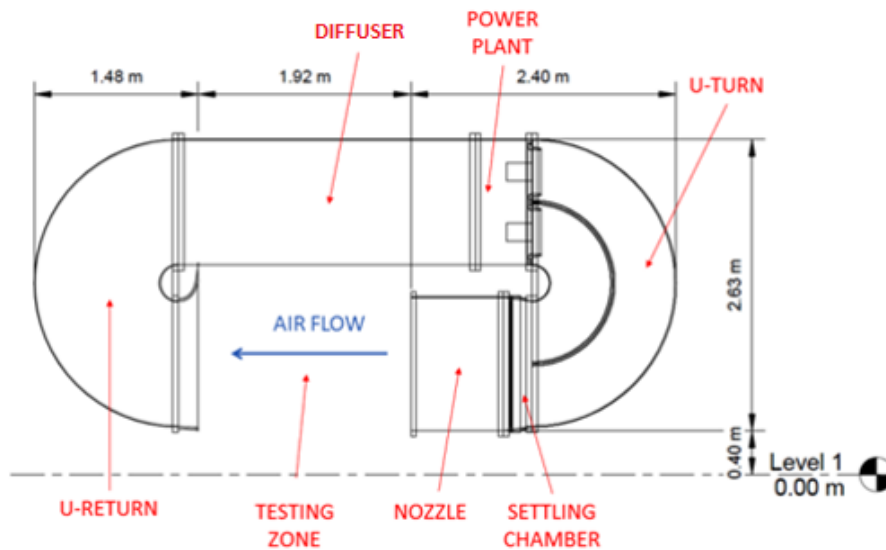


Figure 3.1. The different sections of the one-third scale wind-tunnel in an open jet, closed-circuit configuration.

The one-third scale wind generator is powered by 10 axial fans (280W each) forcing air into individual square ducts that carry the air through a 180 degree arc before combining the flows in the settling chamber. Axial fans were chosen over

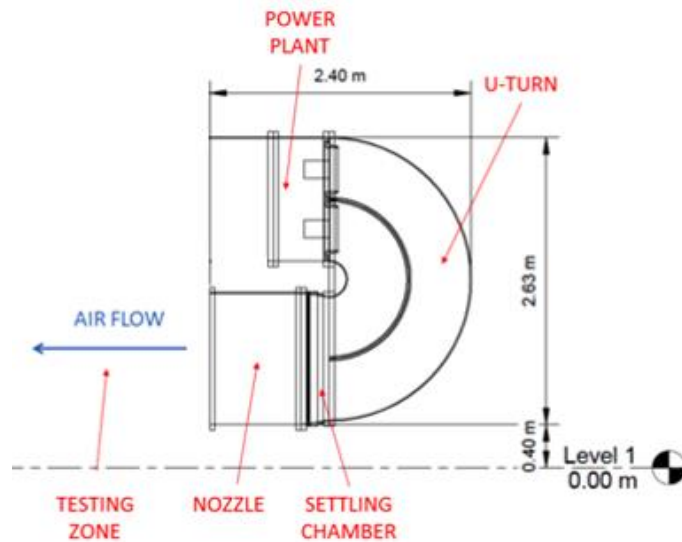


Figure 3.2. The one-third scale wind generation system investigated in this chapter in an open jet, open-circuit configuration.

centrifugal fans to produce high volume wind in a tunnel where large pressure drops were not expected. Upon entering the settling chamber the air will first pass through a section of honeycomb before encountering mesh screen(s). The settling chamber was designed with slots to accommodate square screen frames used to condition the flow of air. These frames completely span the settling chamber and are slid in through the side of the chamber via an access panel. In this work these frames are modified to hold one, two, or, three layers of screen. The screens are supported by a heavy gauge, low blockage structural steel mesh mounted within the same frame. This coarse mesh backs the conditioning screens to support them along their entire span against the drag forces they experience. The nozzle reduces the rectangular cross section exiting the settling chamber to a final section 1.8 m wide by 1.2 m high with fiberglass flow restrictions further reducing the upper corners to filleted radii of 0.5 m as shown in Figure 3.3. This results in a 41%

reduction in the cross sectional area equating to a contraction ratio of 1.7, yielding an approximately 70% increase in mean flow rate and a 30% reduction in turbulence intensity [47].



Figure 3.3. The wind generator fan arrangement and nozzle are shown.

The honeycomb and screens that are installed in the settling chamber will be employed to condition the flow while minimizing pressure losses across each device. The initial configuration of the wind generator included the use of a honeycomb sheet (7.6 cm thickness, 1.25 cm cell width) shortly after the convergence of the 10 square ducts. Immediately downstream from the honeycomb a heavy gauge screen was installed as the structural support for fine mesh screen (wire diameter of 1.52 mm and 3.05 mm opening) that is subsequently added one layer at a time to analyze each layer's effectiveness.

3.2 Results and Discussion

The calculated turbulence strength in the horizontal plane perpendicular to the flow for a sample taken at the mid-section at 0.5 meters from the nozzle can be seen in Figure 3.4. In this figure the expected area in which the turbine is expected to operate and the shear zone can be seen. Low turbulence is sought in the expected area of turbine operation (2-3% in the x direction for this case), with higher turbulence ratios occurring in the shear zone (10-30% in the x direction for this case). Both turbulence values are within the turbulence order of magnitude obtained by de Ridder [40].

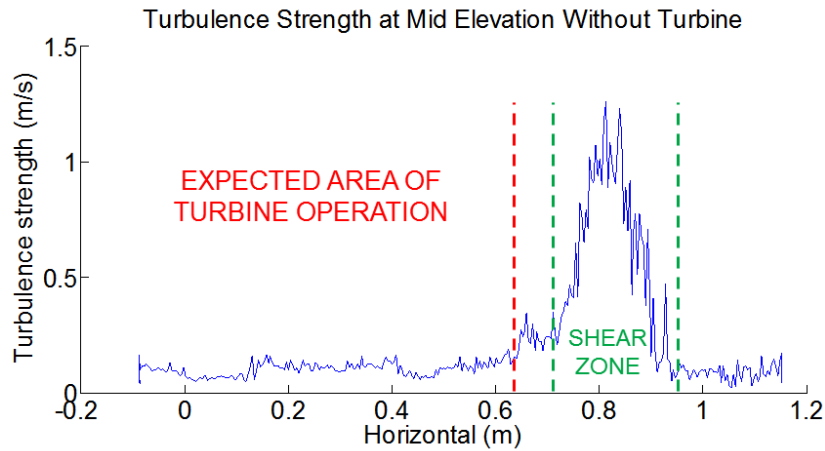


Figure 3.4. A sample of the turbulence strength calculation is shown for a flow of 5m/s at the midsection.

The turbulence created by the system has to be mitigated with the use of honeycomb, several layers of mesh screen, and a nozzle. Although, it is known that adding more screens and honeycomb diminishes the turbulence, it has an adverse effect on the maximum flow speed generated by the wind tunnel [48]. As

such, the first sets of tests were done to evaluate the influence of incrementing the number of screens on the turbulence and flow. The following mean velocity results are calculated by the measurements of the acoustic anemometer. The turbulence intensity is calculated from the standard deviation of the turbulence measurements of the hot wire divided by the acoustic anemometer measurement at each location. The spacing between each contour line for the mean velocity and turbulence intensity are 0.25 m/s and 0.025% respectively.

Figures 3.5, 3.6, and 3.7 show the flow and turbulence at 0.5 meters in front of the nozzle using one, two, and three screens respectively. The projected area of one half the nozzle is shown in the black dashed line in these figures. It can be seen in the surveys above that as each layer of screen is added the variability in the velocity in the central testing area decreases. The velocity becomes more consistent throughout the testing area at the expense of the maximum achievable velocity. In the case of one screen being used, the velocity at the center of the test area was 6.5 m/s and has turbulence intensity of 0.0387 at the center of the nozzle. The addition of a second screen decreases the velocity in the center of the test area to 5.5 m/s and turbulence intensity to 0.0281. A third screen decreases the mean velocity in the center of the test area further to 5.0 m/s with a turbulence intensity of 0.0149 at the center of the nozzle.

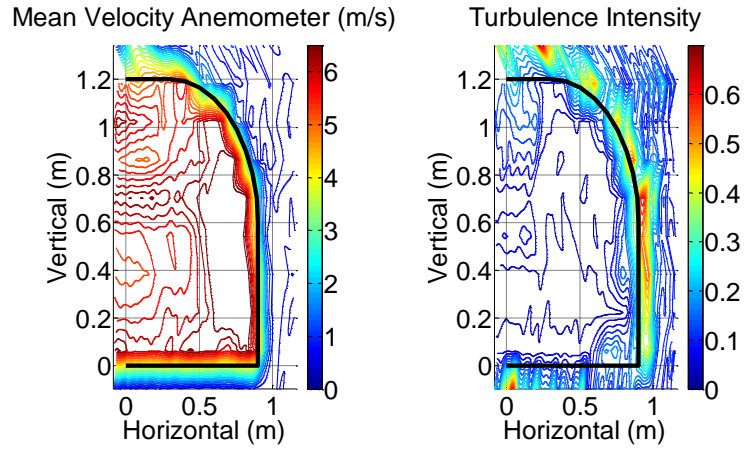


Figure 3.5. Flow field 0.5 m from the nozzle at 5 m/s using one screen.

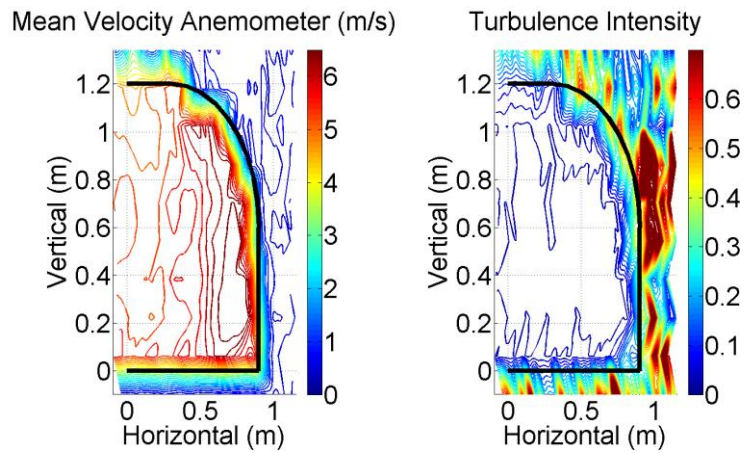


Figure 3.6. Flow field 0.5 m from the nozzle at 5 m/s using two screens.

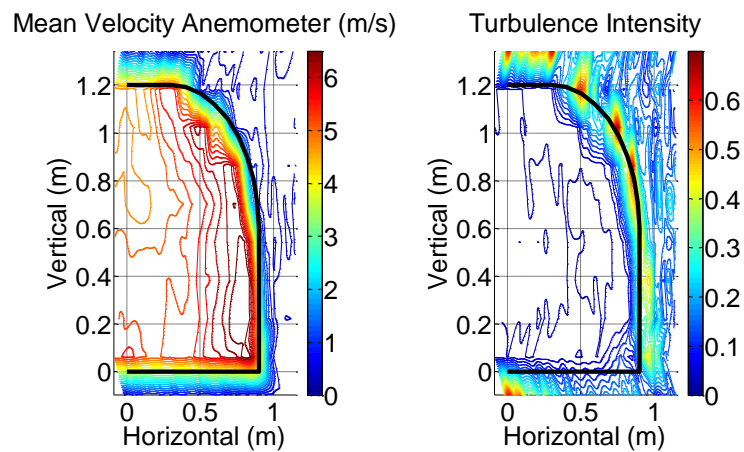


Figure 3.7. Flow field 0.5 m from the nozzle at 5 m/s using three screens.

Additionally this arrangement of screens results in a highly uniform flow field being produced up to 10-20 cm from the projected nozzle perimeter 0.5 m downstream from the nozzle opening. The application of three screens achieves the design requirements of low turbulence and a maximum velocity of 60 m/s in full scale (or 5 m/s at this test scale).

Figures 3.7-3.10 are analyzed to determine the evolution of the flow field from the nozzle. These Figures show the results of the survey throughout the test area starting in Figure 3.7 at 0.5 meters downstream from the nozzle and moving an additional 0.5 meters in each step until a distance of 2.0 meters is reached in Figure 3.10. In analyzing this data, what is most apparent is the evolution of the shear zone, and the contraction of the zone with low turbulence. As the air from the tunnel moves farther downstream from the nozzle the thickness of the shear zone increases. As this shear zone evolves and expands, the measured turbulence intensity decreases as the vorticity dissipates. It can also be seen that the turbulence intensity is lower for the slower air speeds surveyed around the perimeter of the test jet.

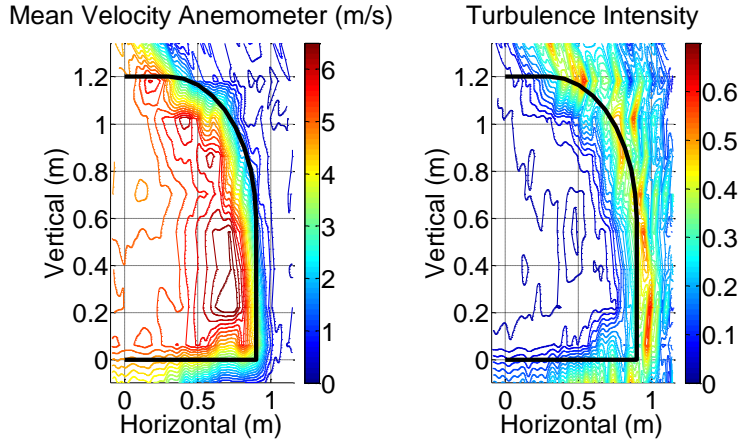


Figure 3.8. Flow field at 1.0 m from the nozzle using three screens with a 5m/s flow at the center point.

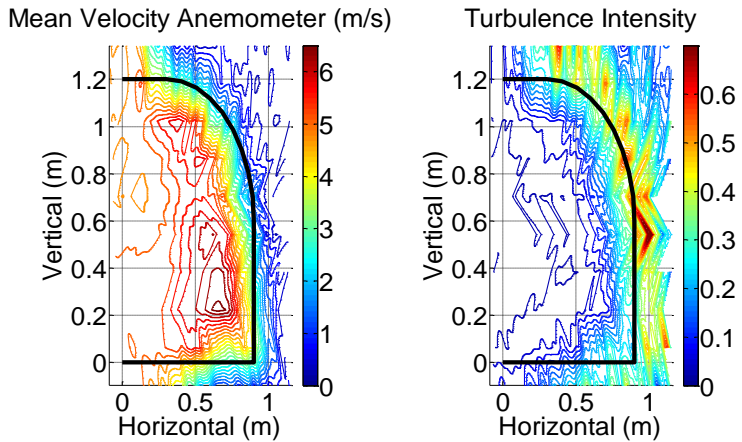


Figure 3.9. Flow field at 1.5 m from the nozzle using three screens with a 5m/s flow at the center point.

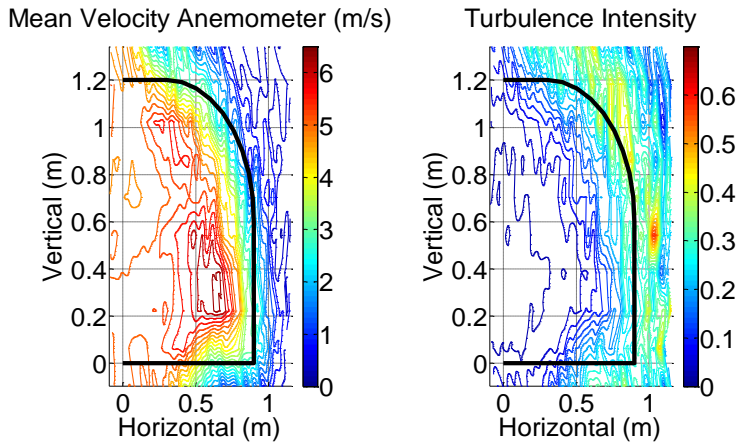


Figure 3.10. Flow field at 2.0 m from the nozzle using three screens with a 5m/s flow at the center point.

It can be seen in Figure 3.7 (0.5 m from the nozzle) that an area of low velocity flow is produced at the top of the test section mid-line. In Figures 3.7-3.10 the deficiency in flow at 0.5 meters is seen to recover by the time the flow has traveled 2.0 m from the nozzle. This deficiency close to the nozzle indicates a separation of flow that may result from one or a combination of two factors; round fans feeding directly into square ducts and a small inner radius of the U-turn section. Any contribution to the low flow in this area from the small radius of the U-turn is expected to be mitigated in the full scale wind generator [49]. Round-to-square diffusers were added between each fan unit and its corresponding square duct to discourage flow separation and the corresponding flow deficiency near the nozzle. The resulting flow profile with the inclusion of these diffusers (Figure 3.11) can be seen to contain less of a flow deficiency at 0.5 meters from the nozzle, in comparison to Figure 3.7. All subsequent wind generator data in this work will reflect the installation of these diffusers.

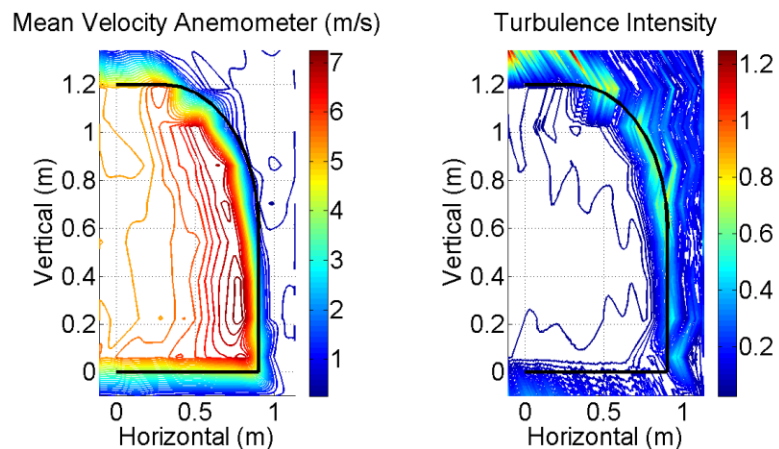


Figure 3.11. Flow field with fan diffusers 0.5 m from the nozzle at 5 m/s using three screens.

A second data set was acquired with and without the turbine operating. This data set was acquired with the wind generator producing a flow of 4 m/s at the midpoint of the nozzle. Figures 3.12-3.15 represent the survey of the wind generator with honeycomb and three screens with no turbine. The mean flow and turbulence intensity are shown in Figures 3.12-3.15 starting at 0.5 meters from the nozzle (Figure 3.12) and moving downstream in 0.5 meter steps to 2.0 meters from the nozzle (Figure 3.15). There is a large field of homogenous flow that extends to within 10-20 cm of the nozzle projection and turbulence is at an acceptable level of 0.07 m/s (turbulence intensity less than 2%), 0.5 meters from the nozzle. The shear zone expands and its turbulent strength decreases as measurements are taken further downstream, as was seen in the data set taken at a flow of 5 m/s at the nozzle midpoint.

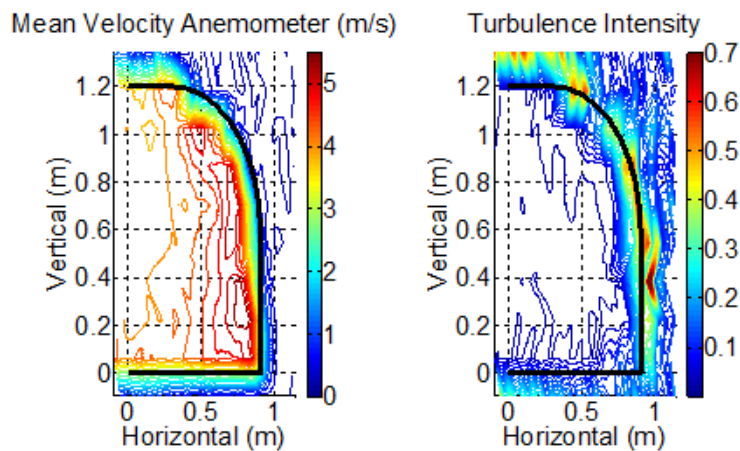


Figure 3.12. Flow field at 0.5 m from the nozzle using three screens with a 4 m/s flow at the center point (no turbine).

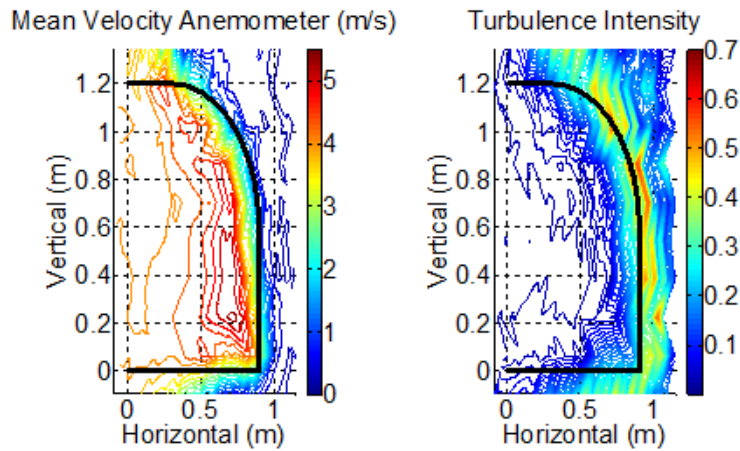


Figure 3.13. Flow field at 1.0 m from the nozzle using three screens with a 4m/s flow at the center point (no turbine).

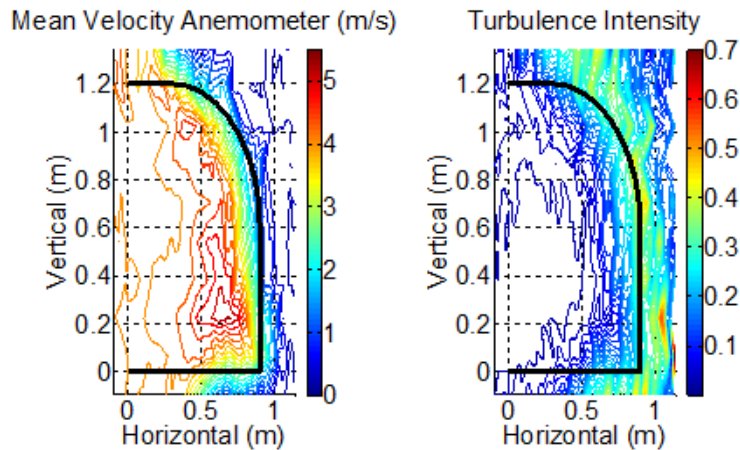


Figure 3.14. Flow field at 1.5 m from the nozzle using three screens with a 4m/s flow at the center point (no turbine).

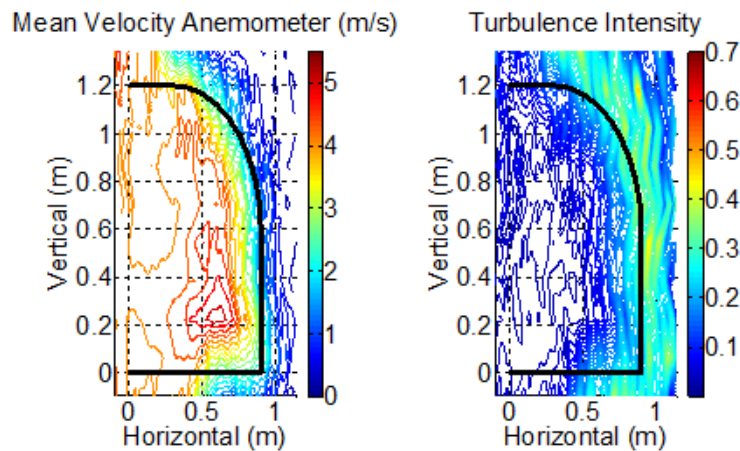


Figure 3.15. Flow field at 2.0 m from the nozzle using three screens with a 4m/s flow at the center point (no turbine).

Figures 3.16-3.20 are a survey of the wind generator under the same flow conditions as Figures 3.12-3.15, with the scaled turbine operating at its maximum power coefficient (Tip Speed Ratio of 7.6). The test turbine was placed at 1.0m from the nozzle. The edge of the turbine swept area is represented by a black dashed line. To avoid interference between the measuring equipment and the turbine's nacelle, measurements were acquired at 0.5 m, 0.75 m, 1.25 m, 1.5 m, and 2.0 m from the nozzle. It can be observed that the turbine induces turbulence and causes a small decrease in wind speed upstream of the turbine (blockage effect) in the operational area. Behind the turbine, areas of induced turbulence can be seen as well (around 0.3-0.4 m/s as compared to 0.1-0.2 m/s without the turbine).

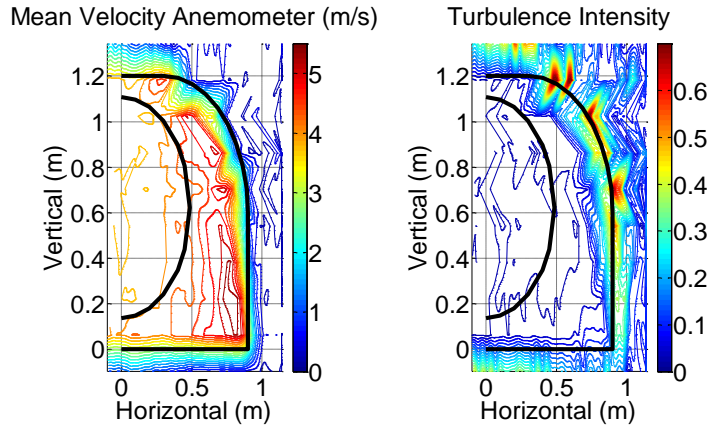


Figure 3.16. Flow field at 0.5 meters from the nozzle using three screens with a 4m/s flow at the center point (with turbine).

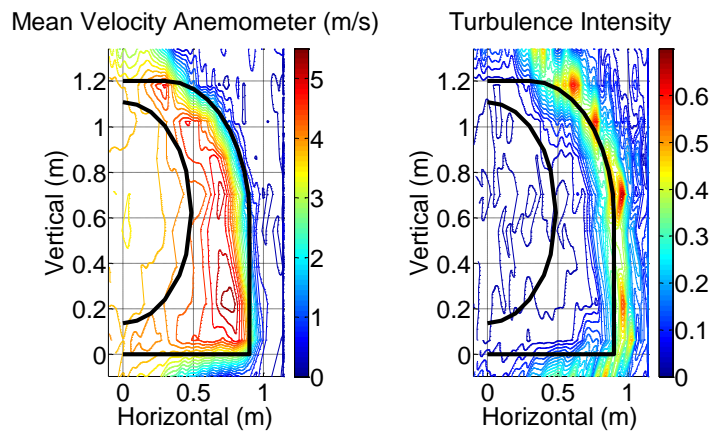


Figure 3.17. Flow field at 0.75 m from the nozzle using three screens with a 4m/s flow at the center point (with turbine).

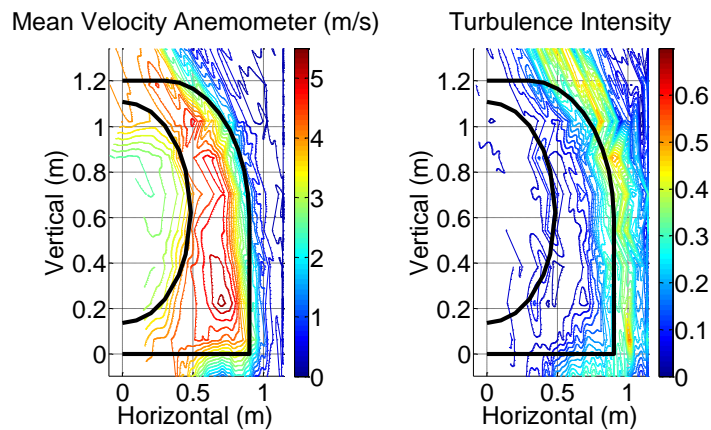


Figure 3.18. Flow field at 1.25 m from the nozzle using three screens with a 4m/s flow at the center point (with turbine).

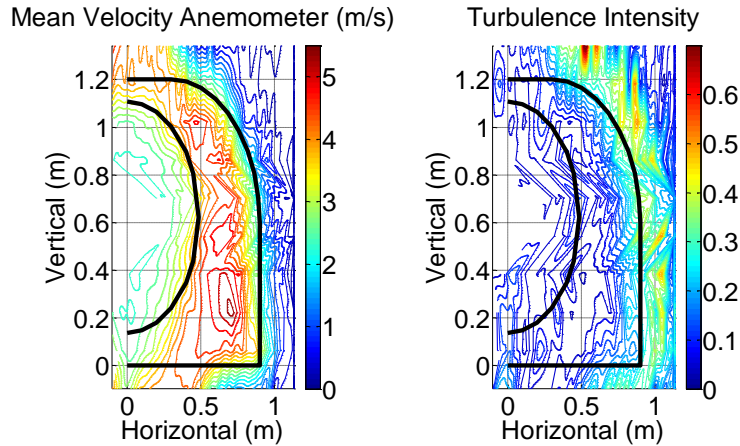


Figure 3.19. Flow field at 1.5 m from the nozzle using three screens with a 4m/s flow at the center point (with turbine).

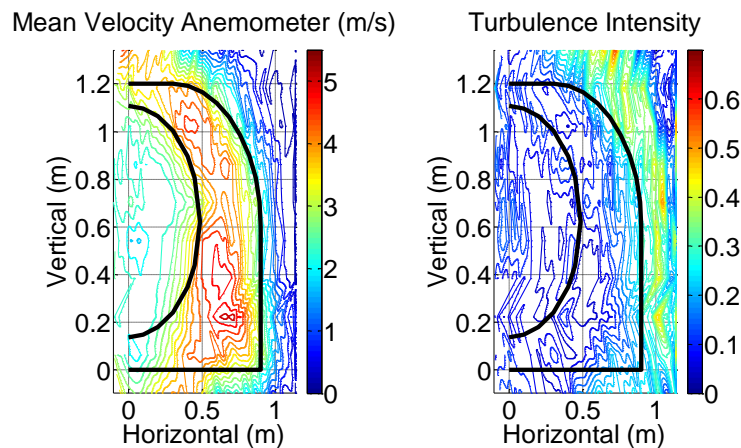


Figure 3.20. Flow field at 2.0 m from the nozzle using three screens with a 4m/s flow at the center point (with turbine).

At 1.5 meters from the nozzle the nominal measurements without the turbine are a velocity of 4 m/s and turbulence strength of 0.13 m/s. At the same location in the shadow of the turbine model the velocity decreased significantly to a velocity of 2.5 m/s in some areas. At the same time the velocity in the test area outside of the projection of the swept area of the turbine shows an increase in

velocity approaching 5 m/s. This indicates that there is an influence on the shear zone expansion, resulting in higher velocity flows that occur at the edge. The turbulence intensity is also greatly increased with the presence of the turbine up to values of 0.1247 where it previously read 0.0369 (at two meters downstream from the center of the nozzle). Figures 3.21 and 3.22 represent a horizontal cross section of the velocities at mid elevation without and with the turbine respectively.

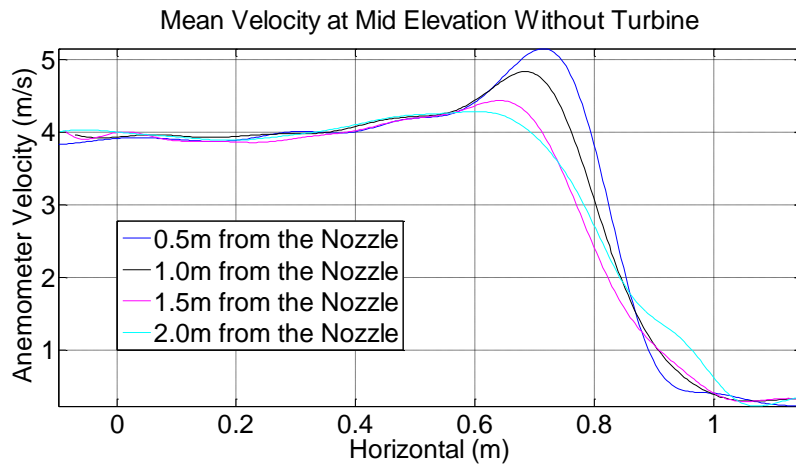


Figure 3.21. Mean velocity at the hub height location without the turbine

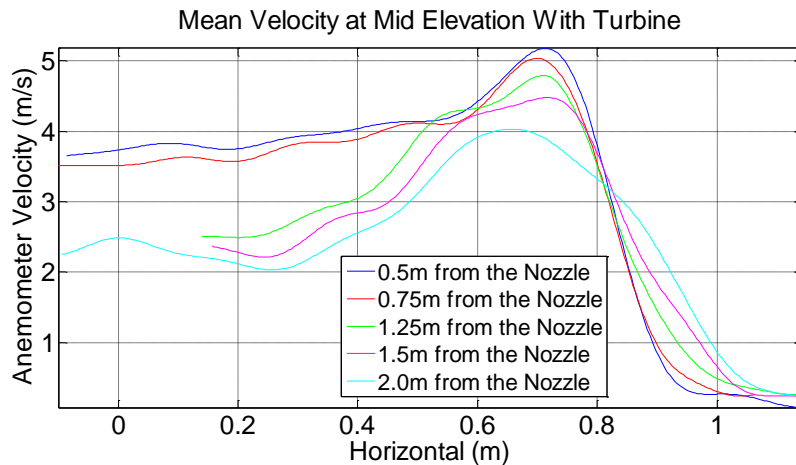


Figure 3.22. Mean velocity at the hub height location with the turbine.

Surveyed data shows a decrease in velocity in the wake of the turbine as would be expected with the conversion of wind to electrical energy by the turbine. The largest decrease in velocity can be seen in comparing the flows with and without the turbine at a distance of 2.0 m from the nozzle opening at around 70% of the blade length.

Figures 3.21 and 3.22 as well as other horizontal cross sections of test data presented later in this work are composed of 300-400 separate points and are therefore a true representation of the velocities along these sections. Section 3 in the chapter to follow will revisit the data shown in figure 3.22 for comparison to data collected in a subsequent trial. At that time the velocities on either side of the turbine will be used to calculate the theoretical power extracted and thrust experienced by the wind turbine as the wind loses energy. This will be of value as it will provide a means to substantiate experimental performance and thrust coefficients measured by the model turbine.

In the chapter that follows the wind generator will be converted to a wind tunnel and investigated for comparison to the baseline data collected and presented in this chapter to explore how tunnel design can impact wind generation capability within a closed building and how turbine performance can vary with tunnel configurations.

Chapter 4

COMPARISON OF WIND GENERATOR AND WIND TUNNEL BEHAVIOR AND THE IMPACT OF NEARBY WALLS ON WIND GENERATOR PERFORMANCE

In this section of work the wind generation system from the previous chapter is converted into a wind tunnel to determine what impact these different configurations have on the quality of wind generated as well as the effect of wind generation type on model turbine experimental results. The wind generation performance in different configurations is compared on the basis of available testing area size, homogeneity of flow, turbulence intensity, and the corresponding power coefficient of a test turbine. A closed-circuit variant of a wind tunnel is considered in these efforts because of the known benefits of similar tunnels over their open-circuit counterparts. Specifically, their ability to control the air that is supplied back into the tunnel makes them immune to changes in orientation within a building. The exact perturbation of wind quality and/or turbine performance in the wind generator due to positional changes within the building is yet unknown. As such, an investigation is launched into the sensitivity of the wind generator during experimental turbine testing to the intrusion of facility walls downstream of the testing section. This sensitivity study is accomplished by placing a wall perpendicular to the flow at different distances downstream of the turbine while monitoring performance characteristics. The wind tunnel configuration could be a viable alternative should the wind generator prove to be vulnerable to influence from nearby facility walls. Alternatively, the use of an active recirculation system

with the wind generator at the end of the test section directly in front of an influencing facility wall could be used to mask the presence of an offending fall. This last configuration is tested in this chapter as well to understand the suitability of a recirculating system as a potential mitigation measure to changes in performance experienced during turbine testing due to proximal facility walls.

4.1 Wind Tunnel Configuration

The wind tunnel is constructed by positioning the U-return facing the U-turn from the wind generation system and connecting the top of these two assemblies with a diffuser as shown in Figures 3.1 and 4.1.



Figure 4.1. Wind tunnel shown in open jet, closed-circuit configuration

At the downstream end of the test section is a collector with a bell shaped opening located in the thickening shear zone that borders the test jet. This collector is tasked with gathering the flow in the test volume and directing it into the U-return.

As discussed in section 1.6, some momentum in the flow is lost here in the outflow of air from the jet as it enters the collector. This loss of flow is compensation for the additional stagnant air that was entrained into the flow through the turbulent mixing in the shear zone surrounding the open jet. The U-return directs the flow up and through a 180 degree bend where it is fed to the diffuser. Any closed-circuit tunnel that employs contraction must also include a diffuser elsewhere in the tunnel. The diffuser enlarges the cross section of the tunnel allowing the air to slow down before it is directed into the fans for reuse.

4.2 Comparison of Wind Generator to Wind Tunnel Flow

The flow of the wind tunnel is surveyed in a similar fashion to previous procedures to see how its performance at full power varies from that of the wind generator (Figures 4.2, 4.3). Figure 4.4 isolates the flow velocity along the vertical centerline for both configurations. In this figure it can be seen that there is a greater velocity achieved with the same power input in the wind generator. Additionally, the wind generator results in a more uniform flow over the wind tunnel which shows a deficit in flow at the top of the tunnel (more on this flow deficiency can be found in Appendix A). Throughout this document wind generator data may appear as “open-circuit” data in some figures. Similarly, wind tunnel data may appear as “closed-circuit” data in some figures.

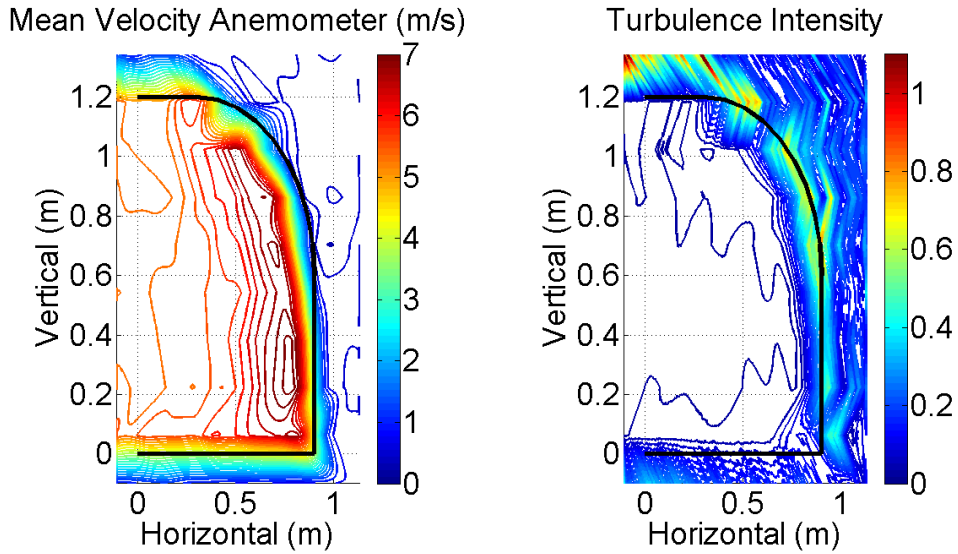


Figure 4.2. Velocity and turbulence profile 0.5 meters from nozzle of the wind generator “open-circuit”.

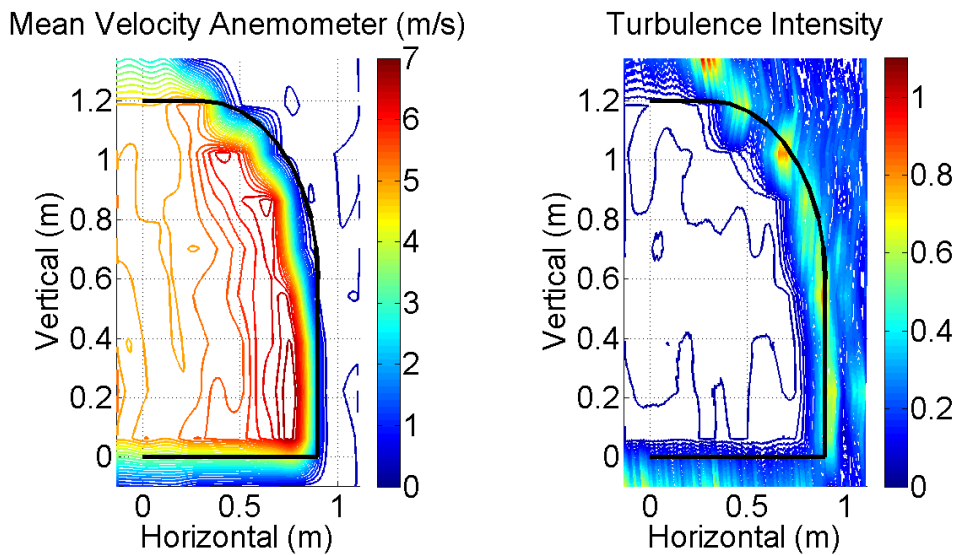


Figure 4.3. Velocity and turbulence profile 0.5 meters from nozzle of the wind tunnel “closed-circuit”.

In Figures 4.2 and 4.3 it can be seen that there is no significant difference in turbulent intensity between the wind generator and the wind turbine. The

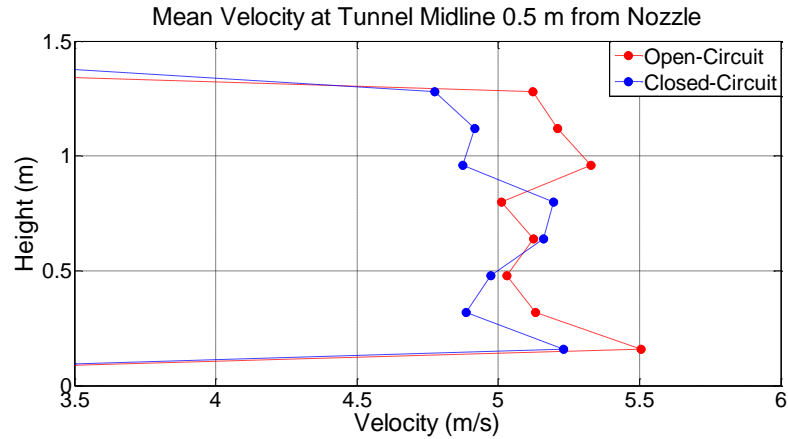


Figure 4.4. Flow velocity along the vertical centerline for both configurations.

majority of the test area is below 5% turbulence intensity for both tunnel configurations and thus each satisfies the turbulence specification established for use in model wind turbine tests. The location of the shear zone however varies from one tunnel configuration to the other. In the wind tunnel configuration the shear zone is closer to the center line of the tunnel than it is with the wind generator, as seen in Figure 4.5.a. The implication of this is that the wind tunnel produces a smaller testable area than its counterpart; this is supported by the mid-elevation velocity surveys seen in figure 4.5.b. When experimental wind turbine testing is conducted in conjunction with a wave basin a FOWT model will not be stationary. It is critical to the success of the test that the rotor remain in the testable area and not encounter the highly turbulent shear zone that surrounds it. As the testable area becomes larger this becomes less of a concern, with the added benefit of being able to accommodate larger scale models.

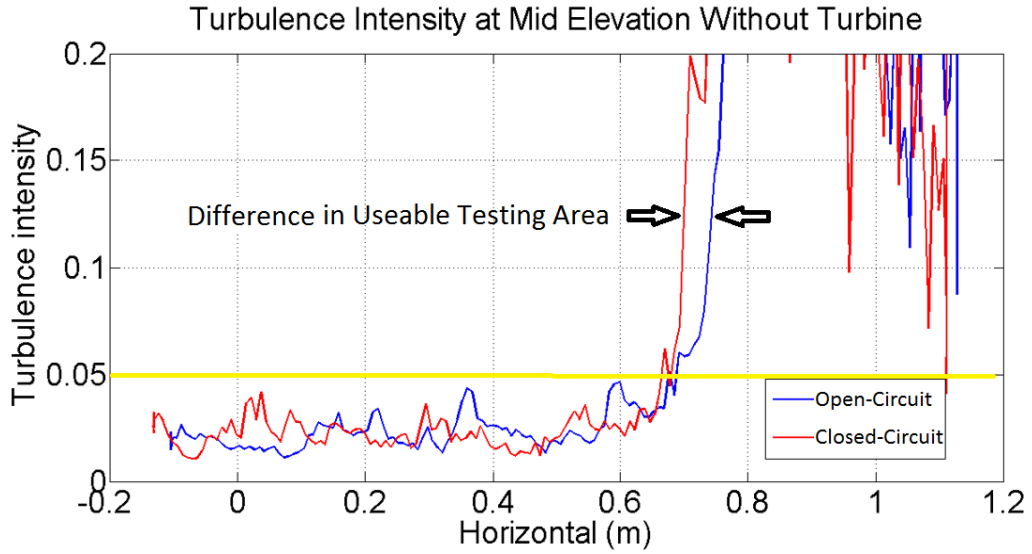


Figure 4.5.a. Turbulence intensities for a mid-elevation tunnel transect 0.5 meters in front of the nozzle at 5 m/s. The yellow line denotes the targeted turbulence intensity. The reduction in the testing area size with the use of the wind tunnel can be seen.

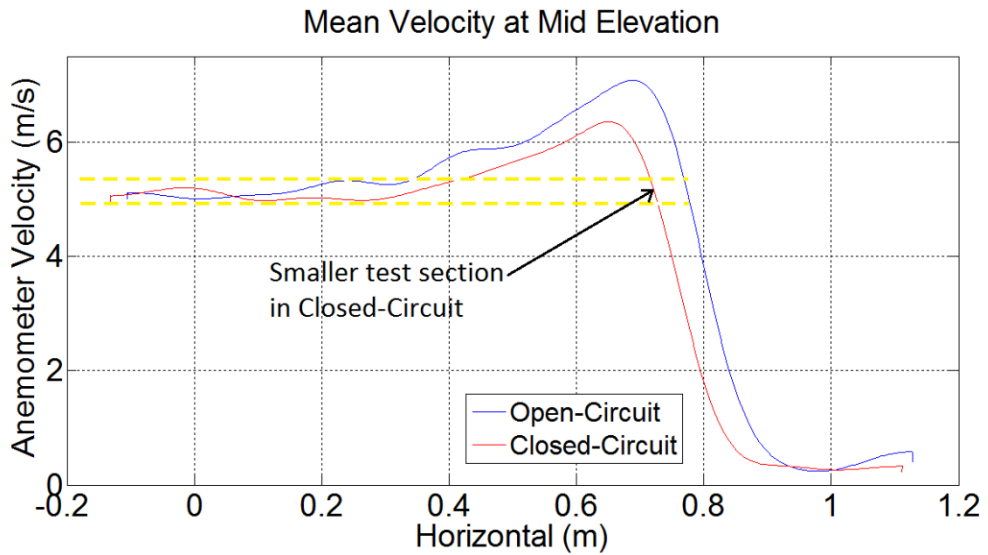


Figure 4.5.b. Velocities for a mid-elevation tunnel transect 0.5 meters in front of the nozzle at 5 m/s. The yellow lines denote the targeted velocity and point to a reduction in the testing area size with the use of the wind tunnel.

That noted, the narrowing of the testable area due to the recirculation of the wind tunnel configuration was not out of line with predictions and is not anticipated to significantly diminish the maximum model size permitted by the W^2 basin. Regarding the cause for the slightly diminished area, it is surmised that it may be due to the low pressure area created in the collector at the end of the test section that is intended to draw in and gather the test flow. As it does, stagnant air surrounding the test section is drawn into the flow narrowing the open test jet.

Any variation in performance of a test turbine placed with the wind generator versus the wind tunnel would be of value to understand before constructing the full scale system. As discussed previously, both configurations operate below the maximum specified turbulence intensity with only nominal differences between the performance of the different configurations, mainly a slightly smaller testable area and a localized deficit of flow in the wind tunnel configuration. The unknown sensitivity of a wind turbine to these different wind tunnel configurations is the motivation for testing the turbine described in section 2.4. In the section that follows the maximum non-dimensional power and thrust coefficient of the turbine will be analyzed in both wind system variants.

4.3 Turbine Performance Comparison from Wind Generator to Wind Tunnel Configuration

In Figures 4.6 and 4.7 a survey of the test area is shown for both wind system configurations 1.5 meters from the nozzle directly behind the test turbine which is located 1 meter from the tunnel nozzle. Comparison of these velocity profiles and turbulence intensity maps show little variation from one configuration to the other save a slight narrowing of the turbine wake with the wind tunnel.

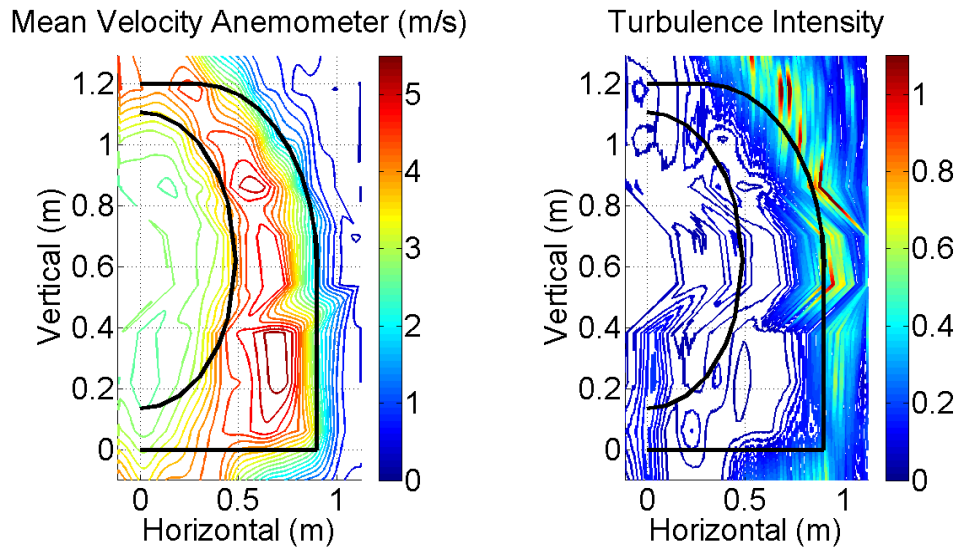


Figure 4.6. Velocity and turbulence 0.5 m behind a turbine placed 1 m from the nozzle of the wind generator operating at 4 m/s.

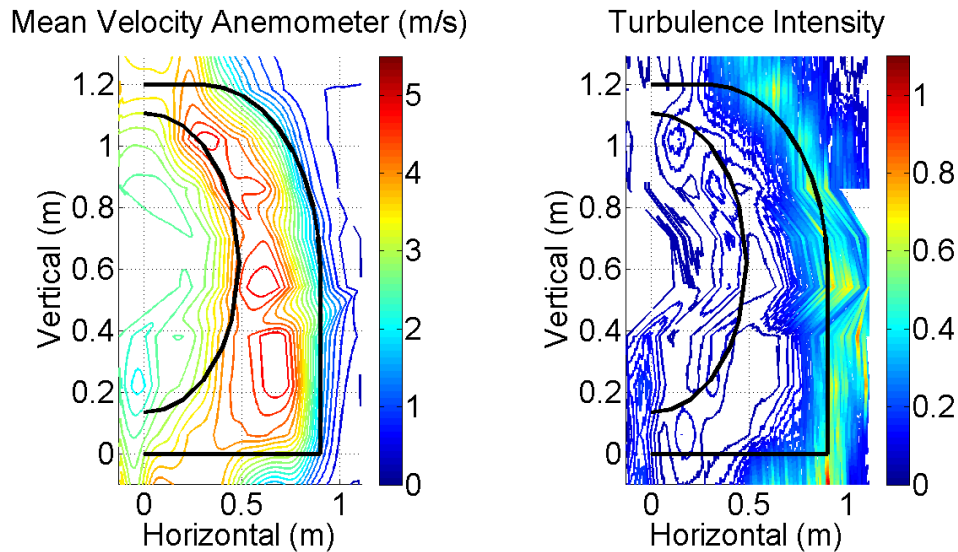


Figure 4.7. Velocity and turbulence 0.5 m behind a turbine placed 1m from the nozzle of the wind tunnel operating at 4 m/s.

Figures 4.8 and 4.9 show the power and thrust coefficients for the turbine operating in both wind systems at a TSR of 7.6 at two different wind speeds. The model turbine returned a power coefficient of approximately 35% in each configuration, for each of the wind speeds tested. Experimental testing of offshore floating wind turbines places a greater importance on thrust rather than power coefficients due to the associated dynamic contributions to the floating structure. Figure 4.9 shows a difference in the thrust coefficient for the two different tunnel configurations with the greatest non-dimensional thrust coefficient measured while the turbine operated in the wind tunnel configuration.

Figures 4.10 and 4.11 show the mean velocities of air flow at the turbine hub height for both wind systems upstream and downstream of the test turbine. In

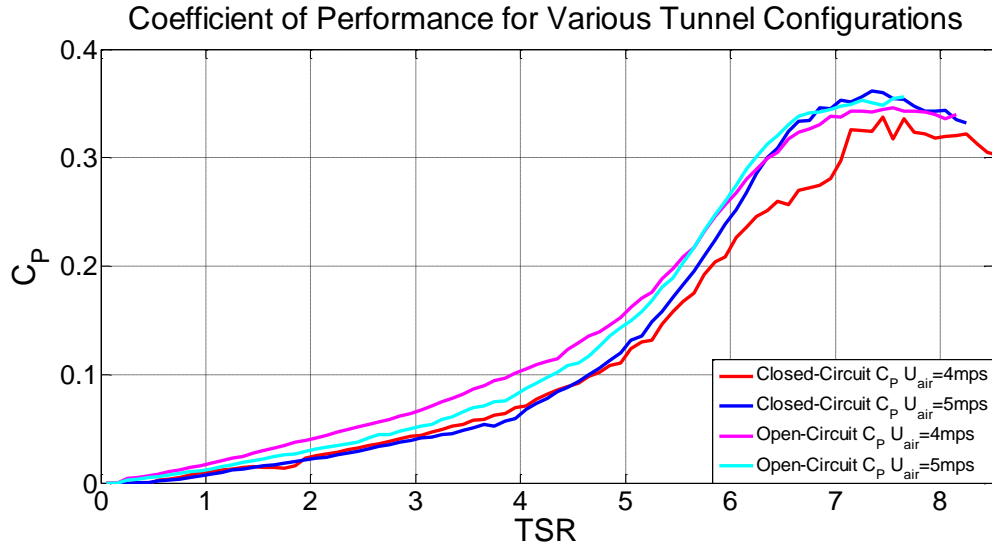


Figure 4.8. Power coefficients for a test turbine operating in both wind systems at various wind speeds.

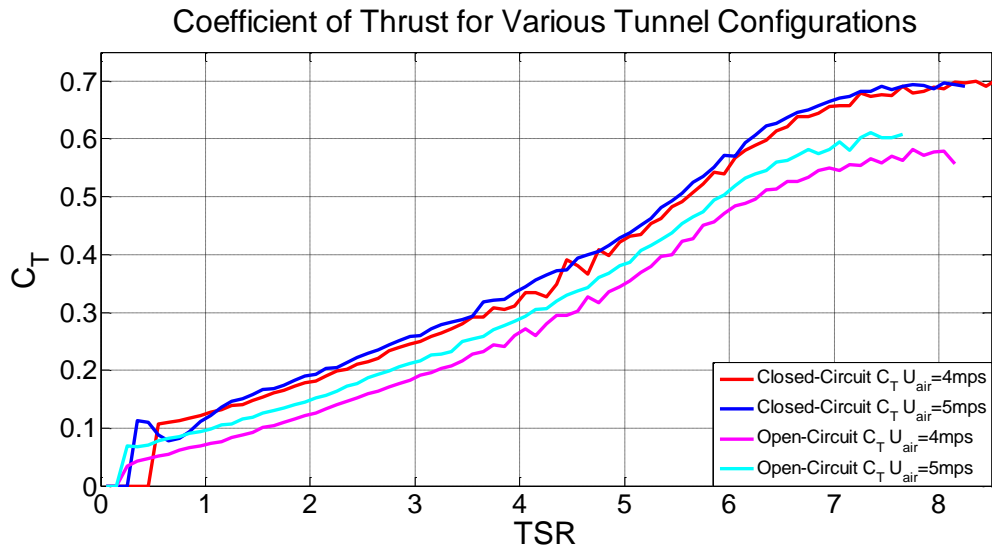


Figure 4.9. Thrust coefficients for a test turbine operating in both wind systems at various wind speeds.

both trials the systems are supplied with the necessary power to generate a flow of 4 meters per second. What is immediately evident is the greater blockage effect over a larger area in front of the turbine in the wind tunnel and the corresponding

lower velocities throughout this vicinity. Additionally, there is a narrowing of the testing area ahead of the turbine in the wind tunnel arrangement. Aft of the turbine a narrowing of the turbine wake and the shear zone bordering the test area is seen in the wind tunnel configuration when compared to the wind generator variant; presumably, this is a result of the negative pressure created at the bell-shaped collector. It was shown in section 3.2 that the turbine's wake caused the shear zone surrounding the test area of the wind generator to expand, while figures 4.5.a-4.5.b and 4.10-4.11 show a contraction of the shear zone caused by the wind tunnel. This points to a conflict between the expansion of the turbine's wake and the narrowing shear zone of the wind tunnel in which the development of the turbine's wake is stunted; this could account for the greater thrust coefficient measured in the wind tunnel configuration. Overall, the flow velocities behind the turbine are less in the wind tunnel configuration; this is confirmed by the velocity and turbulence surveys measured behind the turbine in Figures 4.6 and 4.7. In either configuration, a marked decrease in flow velocity is seen across the turbine as energy is extracted. The velocity data from Figures 4.10 and 4.11 fore and aft of the turbine allow the opportunity to use actuator disk theory (equations 8-11) to calculate the theoretical power coefficients of the turbine in either configuration. The greater differences in upstream and downstream velocities measured in the tests conducted at 4 m/s made these tests better candidates for this investigation. Analysis of upstream and downstream flow velocities predicts a maximum power coefficient of 50% in the open-circuit configuration and a slightly lower 46% power coefficient in the closed-circuit tunnel. This exercise corroborates the greater

turbine performance achieved in the wind generator over the wind tunnel as seen in Figure 4.8. Additionally, these theoretical values support the rationality of the experimental values (approximately 35%) by exceeding them.

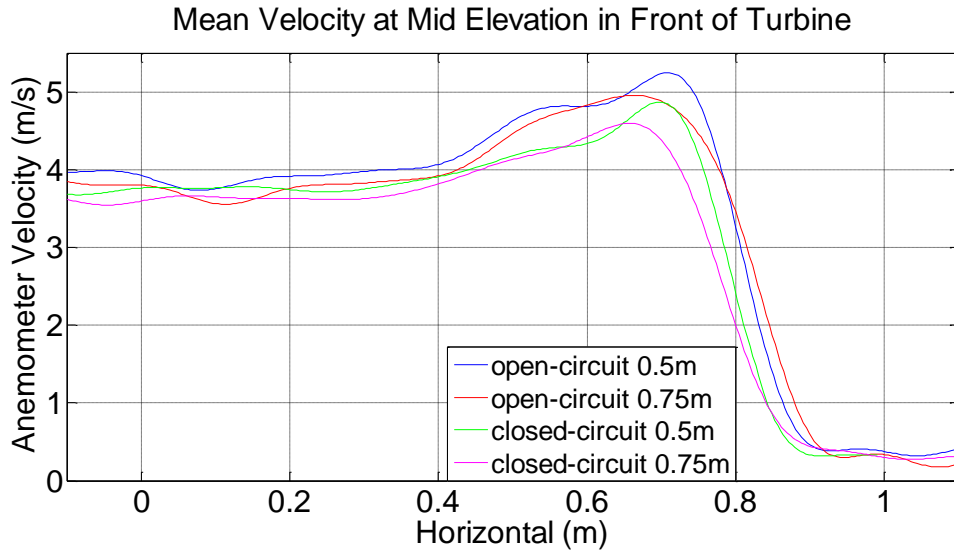


Figure 4.10. Flow at mid elevation in front of test turbine in both wind systems.

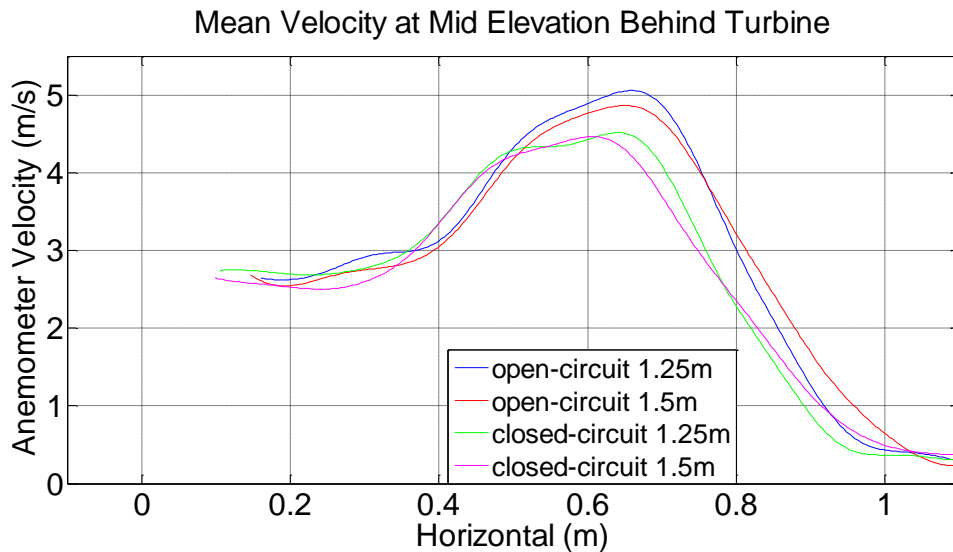


Figure 4.11. Flow at mid elevation behind test turbine in both wind systems.

$$C_T = 4a(1 - a) \quad (8)$$

$$C_P = 4a(1 - a)^2 \quad (9)$$

$$a = \frac{U_\infty - U_R}{U_\infty} \quad (10)$$

$$U_R = \frac{U_\infty + U_w}{2} \quad (11)$$

In equations 8-11 thrust and power coefficients are calculated with the aid of the axial induction factor (a) which is a function of the free-stream velocity (U^∞) upstream of the turbine and the far wake velocity (U_w) downstream of the turbine.

4.4 Facility Wall Effect

In the last exercise, the test turbine's performance in a wind tunnel is compared to its performance with a wind generator without any obstructions downstream of the test turbine; similar to an infinite stream. An infinite stream is an unrealistic expectation for an open-circuit tunnel located within a building that may have walls within close proximity to the tunnel. One of the benefits of a wind tunnel over the wind generator is its ability to control the air that is supplied back into the tunnel. In the design of an enclosed wind-wave facility where the wind system will be rotated through different orientations the wind tunnel has the potential to standardize the flow of air in the test section regardless of its position. This argument was presented in section 1.6 as past tunnel designers have discovered the open-circuit tunnel's susceptibility to performance degradation if its

inlet or exhaust sections are close enough to the structure of the building housing it. The W^2 wind-wave facility building at the University of Maine is rectangular with a length much greater than its width. As such, when the wind system is oriented perpendicular to the wave basin the facility wall downstream of the test section will be significantly closer than when the system is aligned with the wave basin. The choice of wind system used should consider the sensitivity of these systems to the presence of nearby walls. As such, an investigation was launched to determine the impact of the facility's walls on the performance of the wind generator.

An investigation into the effect of proximal building walls on the performance of the wind generator is of particular interest. In the design of the W^2 facility, where the difference in wind systems will have a profound budgetary impact, evidence of the wind generator being insensitive to nearby building walls would be welcomed

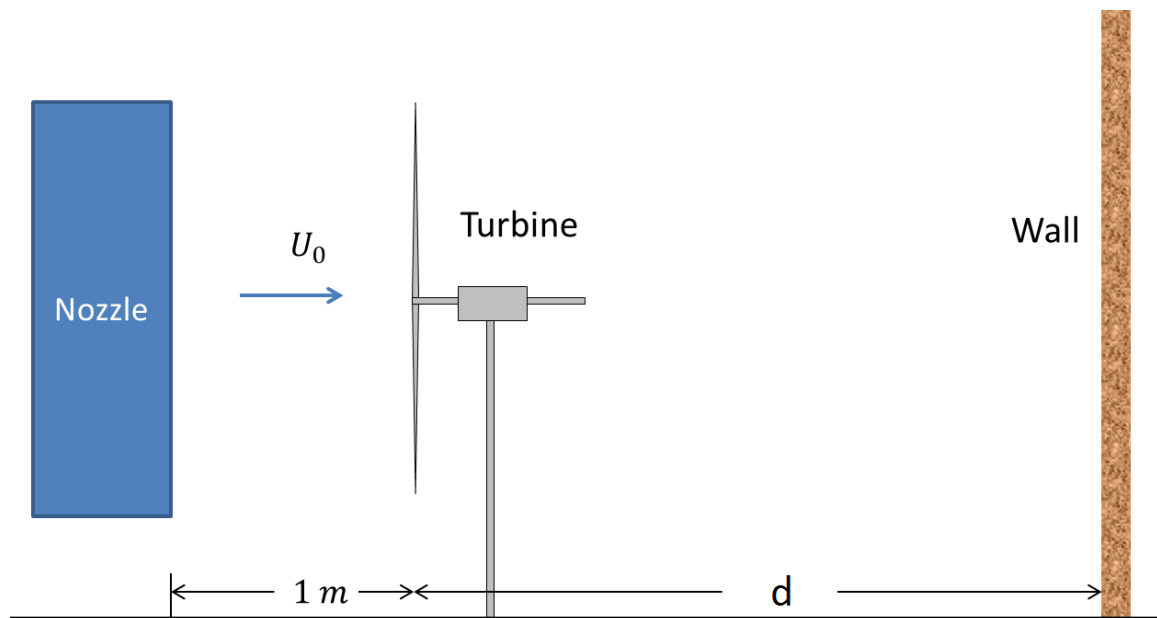


Figure 4.12. Test configuration for the wall sensitivity study.

in a construction project with a limited budget. The test set up of this sensitivity study uses the arrangement seen in Figure 4.12. The performance of the turbine was determined for both wind systems according to the procedures described in section 2.5 at 4 meters per second and 5.4 meters per second, two speeds common to the testing matrix. A wall measuring 3 meters by 3 meters was constructed on site and placed behind the test turbine at various distances measured in turbine diameters (D) to assess the effect on turbine performance. The resulting power and thrust coefficients can be seen in Figure 4.13. In Figure 4.14 the power coefficient has been normalized with respect to the power coefficient of the turbine without an obstruction downstream. It is apparent that the presence of the wall has an adverse effect on the power coefficient of the turbine that is exacerbated with proximity. The impact of the wall on the performance of the turbine is in line with predictions. In the extreme case of a wall being placed directly against the back of the rotor, airflow through the rotor would cease, preventing the rotor from extracting any power from the flow field resulting in a power coefficient of zero. In the same vein, a wall that is sufficiently distant from the rotor downstream, ten rotor diameters in this case, will allow the turbine's wake to develop in a way similar to an infinite free stream. The insensitivity of the turbine's performance to far field disturbances bodes well for the wind generator's use within a rectangular building when aligned with the longer axis of the building. However, caution should be exercised if the wind generator is used for turbine testing when aligned with the shorter axis of the building as performance may suffer. In Figures 4.13 and 4.14 an adverse effect to the performance of the turbine

can be seen whenever a downstream obstruction is within 4-5 rotor diameters of the turbine scaling to a distance of approximately 15 meters in the wind-wave facility.

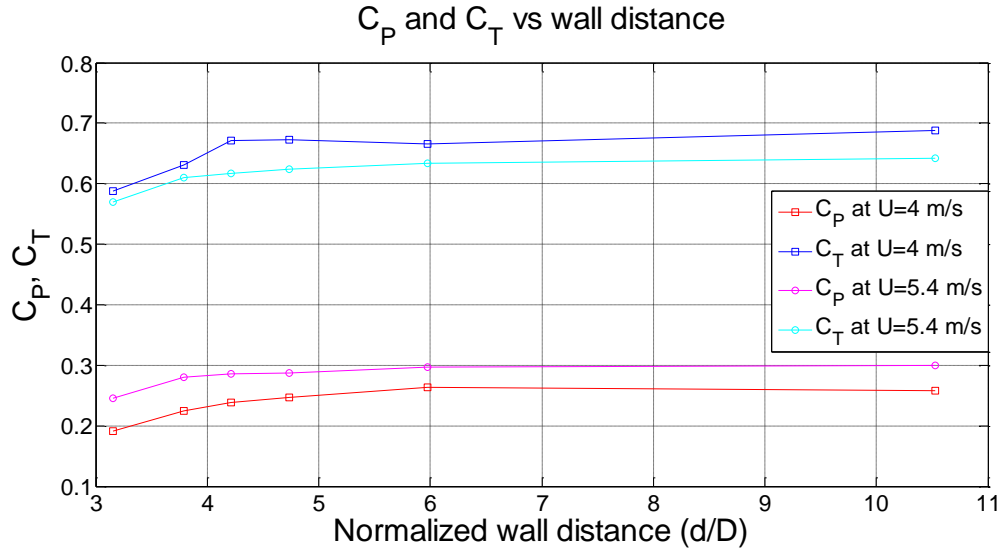


Figure 4.13. Power and thrust coefficients of a test turbine in response to the proximity of a wall perpendicular to the flow, downstream of the turbine

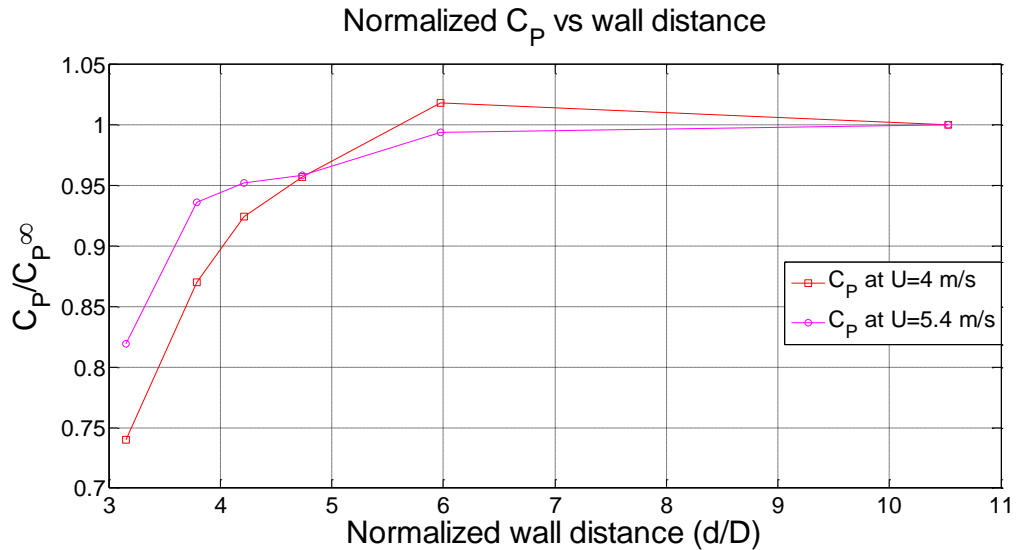


Figure 4.14. Normalized power coefficients of a test in response to the proximity of a wall perpendicular to the flow, downstream of the turbine.

4.5 Active Recirculation

The use of active recirculation with the wind generator was explored as a potential mitigation measure to the negative effect observed from the presence of a wall in the near field of a turbine being tested. In this exploration active recirculation is accomplished by placing a bank of fans at the end of the test section, upstream from any potential perturbing structures as seen in Figure 4.15. The bank of fans is made up of four one horsepower fans arranged in a two by two grid (approximately 1 square meter) with an inclination of 55 degrees from the horizontal. This arrangement does not utilize a duct as the wind tunnel did, but rather collects the air at the end of the test section and accelerates it through the fans at an upward angle due to the inclination of the bank, using the building itself as the return for the system.

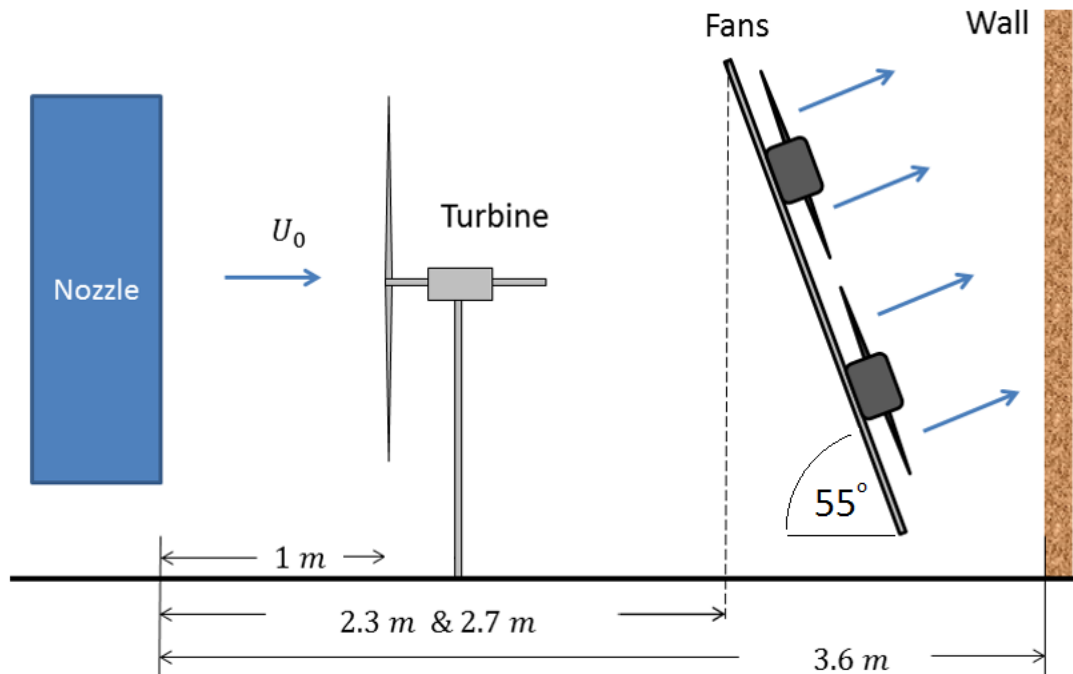


Figure 4.15. Test configuration for the active recirculation effectiveness study.

The results of this active recirculation exploration can be seen in Figures 4.16 and 4.17. In these trials a wall, which had previously diminished the power coefficient of the turbine, was placed perpendicular to the test flow in the near field behind the turbine. The bank of fans producing the active recirculation was placed at two different locations between the turbine and the offending wall and supplied with power varying from 0 to 3kW. The power and thrust coefficients of the turbine were then measured with the wind generator set to produce wind at 4 meters per second. Figure 4.16 shows the actual power and thrust coefficients of the turbine while Figure 4.17 shows these values normalized with the maximum power coefficient and corresponding thrust coefficient of the turbine when operating in a free stream. It can be seen in the figures that follow that the corrective effect of the active recirculation was more effective when placed closer to the test turbine. As expected, the increase of power by the active fans to the system makes it possible to not only match the power coefficient without the wall present, but actually exceed the free stream values. At full scale it would be necessary to determine the amount of power needed to mask the presence of nearby walls by comparing the performance of a turbine in both extreme wind generator orientations with respect to the building. In this investigation 90% of the power used to drive the wind generator was also required by the active return to completely mitigate and mask the negative effects of a nearby wall downstream of the test section.

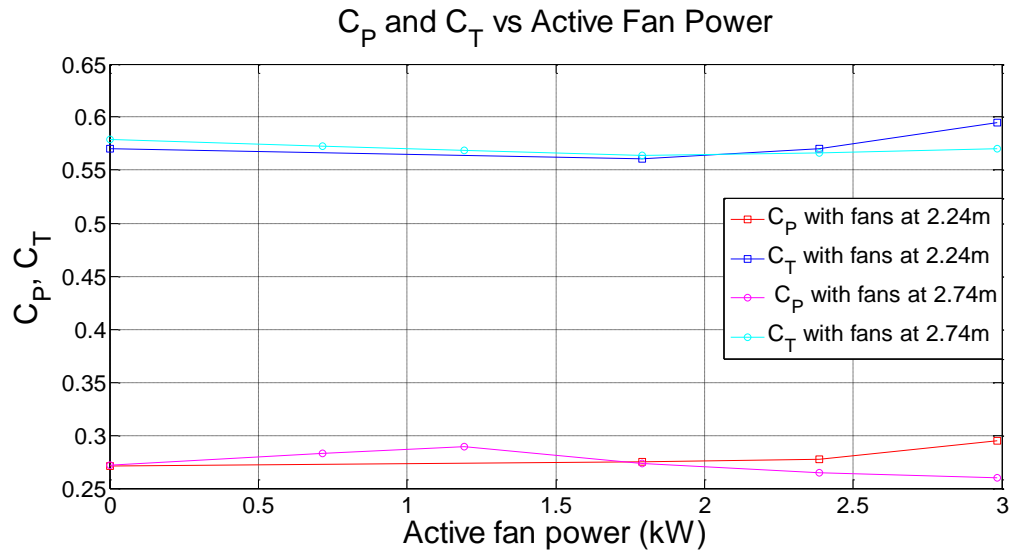


Figure 4.16. Power and thrust coefficients of a test turbine in response to varying power supplied to the active bank of fans.

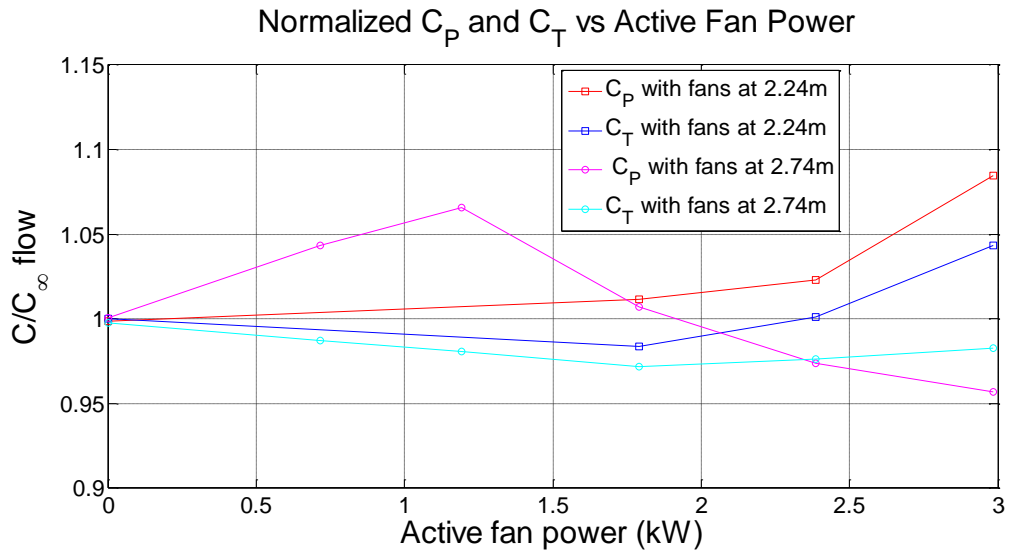


Figure 4.17. Normalized power and thrust coefficients of a test turbine in response to varying power supplied to an active bank of fans.

No significant difference in turbulent intensity was observed from the wind generator to wind tunnel configuration. The main differences between the two wind systems are a slightly smaller testable area and a localized deficit of flow in the wind tunnel configuration. The power coefficient of a wind turbine in both configurations was approximately 35% with a slightly greater non-dimensional thrust coefficient measured in the wind tunnel configuration. In agreement with predictions, it was found that that turbine performance with the wind generator suffered when facility walls were within 4-5 turbine diameters downstream of the turbine. The wind tunnel configuration or a bank of fans used as an active return could be used in these instances to mask the presence of an offending structure wall.

Chapter 5

CONCLUDING REMARKS

The current state of offshore energy research calls for the development of new and improved experimental facilities where wind-wave environments can be suitably replicated. The replication of a quality wind field impervious to the influence of the facility structure is desirable in such a testing environment. Throughout this work the pursuit of quality wind production is outlined in the development of a one-third scale wind system as a testing bed for the full scale system used in the W^2 wind-wave facility.

In the wind generator configuration it was confirmed that the flow could be conditioned with the application of screen mesh to reduce turbulence intensity to meet design specifications while still achieving the required wind speeds and acceptable testing area size. Deficiencies found to exist in the flow were addressed with the addition of diffusers between each fan unit and its respective duct. Although this deficiency in flow may diminish at full scale, due to the larger internal tunnel radius, it is recommended to explore the use of similar diffusers in the W^2 wind-wave facility to aid in flow attachment within the tunnel.

This wind generator was converted to a wind tunnel to assess the differences in testing environments between the two configurations. In doing so, no significant difference in turbulent intensity was observed from one configuration to the other. The majority of the test area produces a wind field below 5%

turbulence intensity in both configurations, and thus, each variation meets the specifications established for use in model wind turbine tests. The main differences between the two wind systems are a slightly smaller testable area and a localized deficit of flow in the wind tunnel configuration. It is hypothesized that this localized deficit of flow at the top of the testing area in the wind tunnel configuration may be a result of air flowing through the small inner radius of the U-return and separating from the tunnel wall as it enters the diffuser. This phenomenon may diminish as the tunnel is scaled up and the inner radius increases and could additionally be mitigated with the inclusion of vanes at the corners of the tunnel to encourage the attachment of flow. At this time little work has been done to optimize the performance of the closed-circuit tunnel and realize its full potential.

This study did not compare the different wind systems on the basis of their dynamic response. However, Matthew Cameron, a test engineer at the University of Maine, has shown that the recirculating tunnel has a greater, or longer, response time than the open jet wind tunnel. Additional work may be warranted in this area should dynamic wind conditions such as gusts be desired in future testing campaigns.

The performance of a wind turbine in both configurations was explored to assess any possible differences. Comparison of the velocity profiles and turbulence intensity maps with a wind turbine show little variation from one configuration to the other save a slight narrowing of the turbine wake and testing

area in the wind tunnel over the wind generator. There was however, a greater blockage effect in front of the turbine in the wind tunnel configuration and correspondingly lower velocities in this vicinity. Despite these differences, the model turbine returned a power coefficient of approximately 35% in each of the wind system configurations at each of the wind speeds tested. There was a slight difference in thrust experienced by the turbine with the greatest non-dimensional thrust coefficient measured while the turbine operated in the wind tunnel.

The wind system used in the W² facility must change its orientation with respect to the wave basin and thus the building to produce a variety of wind-wave conditions without a degradation of wind quality. The wind generator was therefore further investigated to gauge its sensitivity to proximal walls of the structure as it undergoes changes in positioning. In agreement with predictions, it was found that that turbine performance with the wind generator suffered when facility walls were within 4-5 turbine diameters downstream of the turbine. When facility walls are within this influencing distance turbine testing would benefit from the use of a wind tunnel over a similar wind generator.

Active recirculation could be used as a possible mitigation measure to the adverse effects of nearby facility walls downstream of a test turbine in the event that a wind tunnel cannot be used. It was found that a bank of fans used as an active return could mask the presence of an offending structure wall in these

instances. Future work would need to be conducted at scale to determine the exact power requirements of such an active return.

REFERENCES

- [1] Heronemus, W. E. (1972), "Pollution-Free Energy from Offshore Winds," *8th Annual Conference and Exposition Marine Technology Society*, Washington D.C.
- [2] Schwartz, M. (2010) "Assessment of Offshore Wind Energy Resources for the United States," National Renewable Energy Laboratory, NREL/TP-500-45889, Golden, Colorado.
- [3] Jonkman J.M., (2010) "Definition of the Floating System for Phase IV of OC3," *Technical Report NREL/TP-500-47535*.
- [4] Roddier, D., Cermelli, C., Aubault, A., and Weinstein, A. (2010), "WindFloat: A floating foundation for offshore wind turbines," *Journal of Renewable and Sustainable Energy*, Vol. 2, 033104.
- [5] Butterfield, S., Musial, W., Jonkman, J., Scлавounos, P., and Wayman, L. (2005) "Engineering challenges for floating offshore wind turbines," *Copenhagen offshore wind 2005 conference and expedition proceedings*, Danish Wind Energy Association, Copenhagen, Denmark.
- [6] Moon III, WL, Nordstrom, CJ (2010). "Tension leg platform turbine: A unique integration of mature technologies," *Proceedings of the 16th Offshore Symposium, Houston, Texas Section of the Society of Naval Architects and Marine Engineers*.
- [7] Evaluation of internal force superposition on a TLP for wind turbines
By: Adam, Frank; Myland, Thomas; Schuldt, Burkhard; et al.
RENEWABLE ENERGY Volume: 71 Pages: 271-275 Published: NOV 2014.
- [8] Jonkman, J.M, (2007) "Dynamics Modeling and Loads Analysis of an Offshore Floating Wind Turbine," National Renewable Energy Laboratory, NREL/TP-500-41958, Golden, Colorado.
- [9] Nielsen, F.G., Hanson, T.D. and Skaare, B., 2006, "Integrated dynamic analysis of floating offshore wind turbines," *Proceedings of OMAE2006*, Hamburg, Germany.
- [10] The wind from the future - fukushima floating offshore wind farm demonstration project Group Author(s): Hitachi Review Volume: 63 Issue: 03 Pages: 12-17 Published: 2014.

- [11] Building and Calibration of a Fast Model of the Sway Prototype Floating Windturbine By: Hao, Koh Jian; Robertson, Amy N.; Jonkman, Jason; et al. Book Group Author(s): IEEE Conference: International Conference on Renewable Energy Research and Applications (ICRERA) Location: Madrid, SPAIN Date: OCT 20-23, 2013.
- [12] Reference needed. Windsea AS, 2010, "Next Generation Floating Wind Farm," Scandinavian Oil-Gas Magazine, 7/8, pp. 250-253.
- [13] Roddier, D., Cermelli, C., Aubault, A. and Weinstein, A., 2010, "WindFloat: A Floating Foundation for Offshore Wind Turbines," Journal of Renewable and Sustainable Energy, 2, 033104.
- [14] A.M. Viselli, A.J. Goupee and H.J. Dagher, 2015, Model test of a 1:8 scale floating wind turbine offshore in the Gulf of Maine, Journal of Offshore Mechanics and Arctic Engineering 137(4):041901-1.
- [15] Butterfield, S., Musial, W., Jonkman, J. and Scлавounos, P. (2007) "Engineering Challenges for Floating Offshore Wind Turbines," National Renewable Energy Laboratory, NREL/CP-500-38776, Golden, Colorado.
- [16] Jonkman, J.M., (2009), "Dynamics of Offshore Floating Wind Turbines— Model Development and Verification," National Renewable Energy Laboratory, Golden, CO.
- [17] Robertson, A., Jonkman, J., Vorpahl, F., Popko, W., (2014) "Offshore Code Comparison Collaboration Continuation Within IEA Wind Task 30: Phase II Results Regarding a Floating Semisubmersible Wind System," National Renewable Energy Laboratory, NREL/CP-5000-61154, Golden, Colorado.
- [18] Chakrabarti S.K. (1994), "*Offshore Structure Modeling*," World Scientific Publishing Co. Pte. Ltd., Singapore.
- [19] J.M. Jonkman, J.M., and Scлавounos, P.D., (2006), "Development of Fully Coupled Aeroelastic and Hydrodynamic Models for Offshore Wind Turbines," *AIAA Paper 2006-0995, 44th AIAA Aerospace Sciences Meeting and Exhibition, Wind Energy Symposium*, Reno, Nevada, 10-12 January.
- [20] Investigation of a FASTOrcaFlex Coupling Module for Integrating Turbine and Mooring Dynamics of Offshore Floating Wind Turbines Preprint Marco Masciola, Amy Robertson, Jason Jonkman, and Frederick Driscoll To be presented at the 2011 International Conference on Offshore Wind Energy and Ocean Energy Beijing, China October 31 – November 2, 2011.

- [21] Shim, S., Kim, M.H., (2008), "Rotor-Floater-Tether Coupled Dynamic Analysis Of Offshore Floating Wind Turbines", The Eighteenth International Offshore and Polar Engineering Conference, 6-11 July, ISOPE-I-08-384, Vancouver, Canada.
- [22]http://proceedings.ewea.org/annual2011/allfiles2/585_EWEA2011presentation.pdf
- [23] Robertson, A., Wendt. F., Jonkman, J., Popko, W., (2015), "OC5 Project Phase I: Validation of Hydrodynamic Loading on a Fixed Cylinder," National Renewable Energy Laboratory, NREL/CP-5000-63567, Golden, Colorado.
- [24] Bobillier, B., Chakrabarti, S., and Christiansen, P., (2000) "Generation and Analysis of Wind Load on a Floating Offshore Structure", ATCE/OMAE Joint Conference, Energy for the new millennium, New Orleans.
- [25] Buchner, B, Cozijn, H, van Dijk, R, and Wichers, J (2001) "Important Environmental Modelling Aspects for Ultra Deep Water model Tests", Proc Deep Offshore Technology Conference, Rio de Janeiro.
- [26] Courboisa, A., Ferrant, P., Flamand, O., Rousset, J-M., (), "Wind Generation on Wave Tank for Floating Offshore Wind Turbine Applications," Ecole Centrale de Nantes, CNRS UMR6598.
- [27] Khosravi, M, "An experimental study on the near wake characteristics of a wind turbine model subjected to surge, pitch, and heave motions" (2015). *Graduate Theses and Dissertations*. Paper 14367. <http://lib.dr.iastate.edu/etd/14367>.
- [28] Pope, A., (1966), "Low-Speed Wind Tunnel Testing," John Wiley and Sons.
- [29] Bradshaw, P., and Mehta, R. D.,(1979) "Design Rules for Small Low Speed Wind Tunnels," *The Aeronautical Journal of the Royal Aeronautical Society*, pp. 443-49.
- [30] Bradshaw, P., Pankhurst, R.C., (1964) "the design of low-speed wind tunnels," National Physics Laboratory, Teddington, England
- [31] Rajaratnam, N. 1976. Turbulent jets. Vol. 5. Elsevier Science Ltd.
- [32] Thiagarajan, R. Kimball, A. Goupee and M. Cameron, Design and development of a multi-directional wind-wave ocean basin, Proceedings of the Texas Section of the Society of Naval Architecture and Marine Engineers 19th Offshore Symposium, Houston, Texas, USA, February 6, 2014.

- [33] Mehta, R.D., Aspects of the design and performance of blower tunnel performance, PhD Thesis, Imperial College, University of London, 1978.
- [34] Kimball, R.W., Goupee, A.J., Coulling, A.J., Dahger, H.J., (2012), "Model Test Comparisons of TLP, Spar-buoy and Semi-submersible Floating Offshore Wind Turbine Systems," *Transactions of the Society of Naval Architects and Marine Engineers*, Vol. 120.
- [35] Eric-Jan de Ridder, FP7 Program DeepWind – Model test vertical wind turbine, data report, report no. 24662-1-0B Volume II, March 2013.
- [36] Paulsen, U.S., Pedersen, T.F., Madsen, H.A., Enevoldsen, K., (2011), "DeepWind an innovative wind turbine concept for offshore," The European Wind Energy, Annual Conference, 2011, Brussels, Belgium.
- [37] Robertson, A.N., Jonkman, J.M., Masciola, M.D., Molta, P., Goupee, A.J., Coulling, A.J., (2013), "Summary of Conclusions and Recommendations Drawn from the DeepCWind Scaled Floating Offshore Wind System Test Campaign," National Renewable Energy Laboratory, NREL/CP-5000-58076, Golden, Colorado.
- [38] Courbois, A., Flamand, O., Toularastel, J-L., Ferrant, P., Rousset, J-M., (2011), "Applying relevant wind generation techniques to the case of floating wind turbines," 6 th European and African Wind Engineering Conference, Nantes, France.
- [39] Sælen, L., Khalil, M., (2013), "Near and far wake validation study for two turbines in line," The European Wind Energy, Annual Conference, 2013, Vienna, Austria.
- [40] de Ridder, E.J., Otto, W, Zondervan, G.J., Juijs, F., and Vaz, G. (2014) "Development of a scaled-down floating wind turbine for offshore basin testing," *Proc 33rd ASME Int Conf on Ocean, Offshore and Arctic Eng*, San Francisco, California.
- [41] Thiagarajan, K. P., Kimball, R., Goupee, A., Cameron, M. (2014) "Design and development of a multi-directional wind wave ocean basin", *Proceedings 19th Offshore Symposium*, Texas Section of SNAME, Houston, USA.
- [42] <http://www.dantecdynamics.com/docs/support-and-download/research-and-education/probepost.pdf>.

- [43] Kimball, R, Goupee, AJ, Fowler, MJ, de Ridder, E-J and Helder, J (2014). "Wind/wave basin verification of a performance-matched scale-model wind turbine on a floating offshore wind turbine platform," *Proc 33rd ASME Int Conf on Ocean, Offshore and Arctic Eng*, San Francisco, California.
- [44] Navqvi, S.K., 2012, *Scale model experiments on floating offshore wind turbines*, Dissertation, Worcester Polytechnic Institute.
- [45] Farrell, C., Youssef, S., (1992), *Experiments on Turbulence Management Using Screens and Honeycombs*, University of Minnesota, Project Report No. 338, Minneapolis, Minnesota.
- [46] B.J. Koo, A.J. Goupee, R.W. Kimball and K.F. Lambrakos, 2014, Model tests for a floating wind turbine on three different floaters, *Journal of Offshore Mechanics and Arctic Engineering* 136(2):020907-1.
- [47] Batchelor, G.K (1953), *The Theory of Homogeneous Turbulence*, Cambridge University Press, 1953.
- [48] Barlow, J., Rae, W., and Pope, A. (1999), *Low Speed Wind Tunnel Testing*, John Wiley and Sons.
- [49] McDonalogue, D.J., and Srivastava, R.S. (1968), "Motion of a fluid in a curved tube", *Proc. Roy. Soc. A.*, Vol 307, pages 37-57.

APPENDIX A: FLOW SEPARATION

Figures 4.2-4.4 point to a location of diminished flow in the wind tunnel configuration in front of the nozzle at the top of the test section's midline. In comparing the wind tunnel and wind generator performance it can be seen that the homogeneity of flow in the wind tunnel configuration suffers some in comparison with its counterpart. Section 1.6 of this work discussed the ability of the wind tunnel to control and condition the return flow to the tunnel as a benefit over the wind generator's sensitivity to wind gusts and interference from the building's structure. What is observed in this case however is a degradation of performance with the conversion of the wind generator to a wind tunnel. Streamers were installed in the diffuser before the fan units along its walls, floor, and mid volume to get a sense of the nature of flow within the tunnel during operation. In Figure A. the telltale streamers mounted on each wall give an indication of the type of flow that exists within the duct. In the upper region of the diffuser the flow behaves as predicted with the streamers showing a net flow returning to the fan units. The streamers headed away from the fan in the bottom half of the tunnel indicate counter flow and the limits of a recirculation bubble that exists at this location. The frame on the left shows the tunnel operating at a slower speed than the frame on the right. As such, it can be seen that a higher velocity flow results in a larger recirculation bubble. This bubble was highly unstable, when reviewing video taken in the same location, the boundaries of this bubble could be seen to migrate up and down the walls of the tunnel showing changes in its size that were not linked to changes in tunnel flow velocity. Lastly, it was noted that the development of the bubble was not

predictable, the presence of the bubble at a certain tunnel velocity was dependent on how quickly that tunnel velocity was approached.

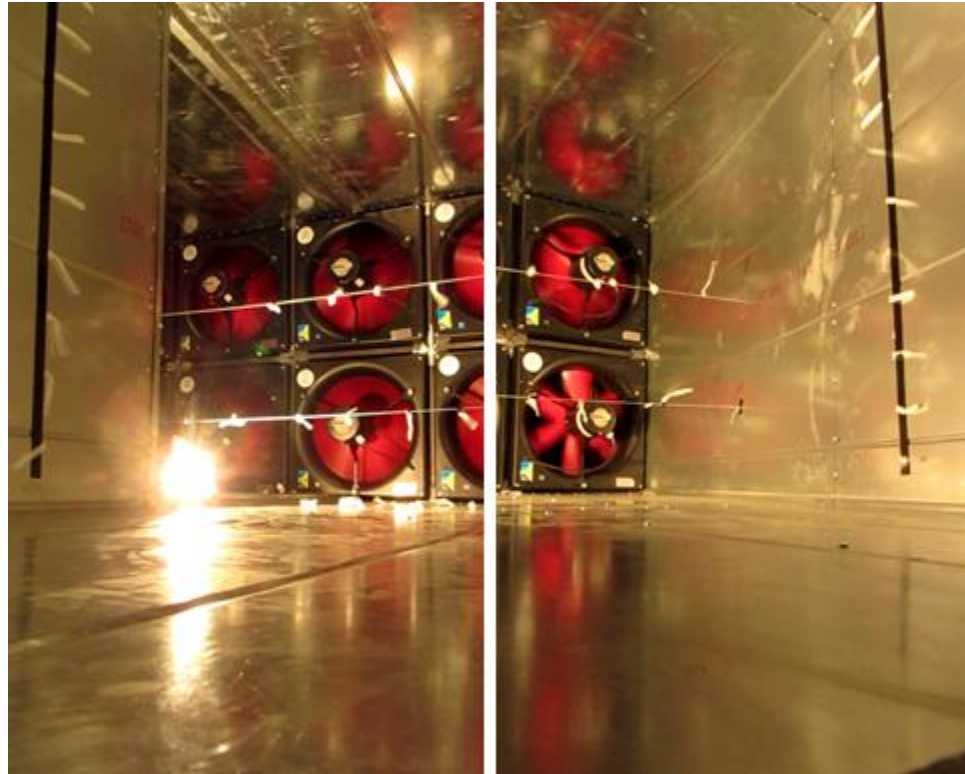


Figure A.1. Behavior of streamers installed on the vertical walls of the diffuser as viewed along the downstream direction.

Figure A.2 shows the possible flow environment within the diffuser that would support the behavior witnessed by the telltale streamers with flow in the net direction at the top of the diffuser and contraflow along the bottom of the diffuser. This separation is first observed in the beginning of the diffuser and continues to develop over the length of the diffuser before being fed back into the fans. It is hypothesized that this separation results from the small (approximately 10cm) inner radius of the U-return. Wind tunnel designers are well aware of this issue and have had success using vanes within the tunnel to abate this separation. In Figures

1.4 corner vanes can be seen in use across the entire tunnel to assist in the change of flow direction. In Figure 1.5 vanes are used near the inner radius of the tunnel curves as a targeted correction that may be more appropriate for the type of separation observed in these tests. At full scale the radius of the tunnel will be larger and the diffuser will be longer, two variables that may improve the amount of separation and corresponding turbulence fed back into the fans. Increasing the overall size of the tunnel may help in correcting this issue but at the expense of additional physical space and costs, both of which may be limiting factors.

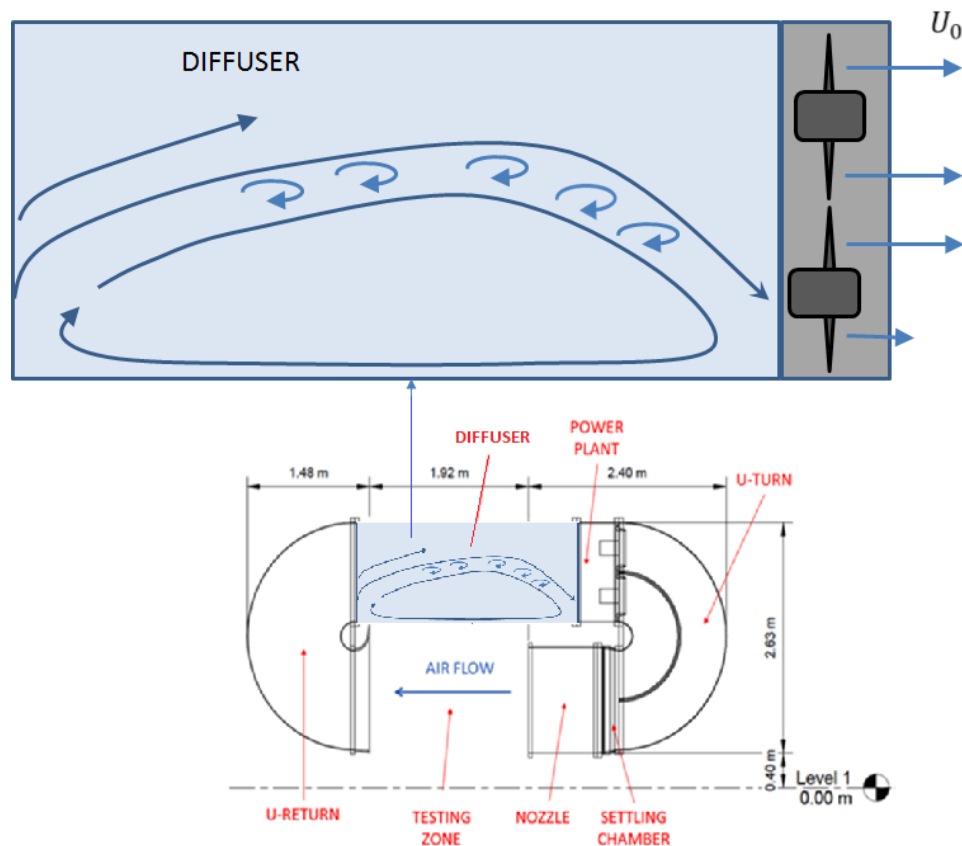


Figure A.2. Visualization of separation within the return section of the wind tunnel.

APPENDIX B: UNCERTAINTY ANALYSIS

In this section the uncertainty (w) of key quantities considered in this work will be analyzed. The uncertainties of the calculated quantities C_P , C_T , U and $T.I.$ are a result of the uncertainties of each of the measured quantities that influence them. As such, the uncertainty of each measured quantity must be known. Final uncertainty of each calculated quantity will be assessed at the values measured for the greatest C_P encountered in this body of work.

Torque values used in C_P calculations were measured by the T2 Precision Rotary Torque Transducer supplied by Interface Inc., which has a specified error of $\pm 0.001\%$. Therefore, the uncertainty of the torque sensor ($w_{\bar{Q}}$) used in this exercise will be 0.1% of the torque experienced at the maximum C_P or $w_{\bar{Q}} = 0.000252 \text{ Nm}$.

Angular velocity is measured with an Analog Encoder supplied by US Digital. This device has a resolution of 1024 measurements for every rotation. The uncertainty of this measurement is then equal to $\frac{1}{2}$ of the smallest increment measureable by the device or $w_{\omega} = \frac{1}{2} \frac{1}{1024} 2\pi = 0.00307 \text{ rad}$.

Air density in the lab varied with pressure, humidity, and temperature resulting in an average density of 1.217 kg/m^3 . The uncertainty used in this analysis comes from the difference between the mean value and the most extreme value measured or $w_{\rho} = 0.0215 \text{ kg/m}^3$.

Area swept out by the turbine in a function of the radius, which was measured manually. The uncertainty of this length measurement is equal to $\frac{1}{2}$ of the smallest measureable increment or 0.0005 m . Therefore the measured radius

of 0.486m with an uncertainty of +/- 0.0005m results in a calculated swept area of 0.742m² +/- 0.00153m² or $w_A = 0.00153\text{m}^2$.

Mean wind speed was measured with a hot wire anemometer with a factory specified uncertainty of 0.05 m/s. This is contingent on the operator orienting the hot wire probe appropriately as the probe is only sensitive to components of wind in the plane perpendicular to the wire element. Geometrically it is found that the probe's experimental error from the true value increases from 0.4% to 1.5% to 3.5% as the probes misalignment increases from 5° to 10° to 15°. With confidence that the hotwire probe was within 5° of its intended orientation an error of 0.4% or 0.02 m/s at maximum wind speed brings the total uncertainty of this measurement up to $w_U = 0.07$ m/s.

Thrust was measured with an AMTI FS6 sensor with an error of 0.2% or $w_T = 0.0147$ N at the maximum thrust value recorded.

Final uncertainties for C_P and C_T can be found with the following.

$$w_{C_P} = \sqrt{\left(\frac{\partial C_P}{\partial \bar{Q}}\right)^2 (w_{\bar{Q}})^2 + \left(\frac{\partial C_P}{\partial \omega}\right)^2 (w_{\omega})^2 + \left(\frac{\partial C_P}{\partial \rho}\right)^2 (w_{\rho})^2 + \left(\frac{\partial C_P}{\partial A}\right)^2 (w_A)^2 + \left(\frac{\partial C_P}{\partial U}\right)^2 (w_U)^2}$$

$$w_{C_T} = \sqrt{\left(\frac{\partial C_T}{\partial T}\right)^2 (w_T)^2 + \left(\frac{\partial C_T}{\partial \rho}\right)^2 (w_{\rho})^2 + \left(\frac{\partial C_T}{\partial A}\right)^2 (w_A)^2 + \left(\frac{\partial C_T}{\partial U}\right)^2 (w_U)^2}$$

Substituting in the uncertainties of each measured value and evaluating the partial derivatives of C_P and C_T at the greatest C_P encountered in this body of work yields a $w_{C_P} = 1.63\%$ and $w_{C_T} = 2.17\%$. Turbulent intensity is the standard deviation of the mean wind speeds and therefore a measure of the wind speed uncertainty found earlier to be $w_U = 0.07$ m/s.

BIOGRAPHY OF THE AUTHOR

James Newton was born in Danbury and raised in Litchfield County, CT. He graduated from WAMOGO Regional High School in 1998. He enrolled at Rensselaer Polytechnic Institute and earned a Bachelor of Science degree in Mechanical Engineering in 2002. James worked in the field of construction as a project engineer for Whiting-Turner and later as the proprietor of a small finish carpentry business. In 2006 he completed a certificate program allowing him to become a High School Physics teacher in East Haven, CT. In 2013 James joined the University of Maine where he has served as a Teaching Assistant and conducted research pertaining to the development of a scale wind tunnel for use in the offshore wind energy industry. He is a candidate for the Master of Science degree in Mechanical Engineering from the University of Maine in May, 2016.